IMPACT OF TURBULENCE ON HURRICANE INTENSITY FORECASTING

SOPAN ANANTHA KURKUTE

A THESIS SUBMITTED TO

THE FACULTY OF GRADUATE STUDIES

IN PARTIAL FULFILMENT OF THE REQUIREMENTS

FOR THE DEGREE OF

MASTER OF SCIENCE

GRADUATE PROGRAM IN

EARTH, SPACE AND ATMOSPHERIC SCIENCES

YORK UNIVERSITY

TORONTO, ONTARIO

December, 2014

Abstract

Hurricane intensity prediction and track forecasts are very sensitive to turbulence within the Hurricane Boundary Layer (HBL). In the Advanced Research Weather Research and Forecasting (WRF-ARW) model the effect of the sub-grid scale (SGS) turbulence can be represented by varying the magnitude of the model grid-size (Δx) and Smagorinsky constant (C_s). The effect of turbulence on the hurricane intensity has been investigated by simulating Hurricane Danielle (2010) using WRF-ARW model. The properties and characteristics of the turbulence within the HBL has been investigated by a Large Eddy Simulation (LES) of the idealised Hurricane using WRF. The kinetic energy spectra computed for a high-resolution domain of grid-size $\Delta x = 62m$ showed that the size of the maximum energetic turbulent eddies lies between 700m-3000m and matches well with the estimated horizontal turbulence mixing length scale $L_h \approx 750m - 1500m$. Defining a filter scale of $\approx 1.5km$ matching with the resolution of the current hurricane forecast models, the flow in the HBL was spectrally decomposed into the filter scale and sub-filter scale (SFS) motions. The SFS turbulent motions were then used for diagnosing the turbulence properties within HBL. The estimated Turbulent Kinetic Energy (TKE) budget shows that shear production is the dominant mechanism for generating turbulence, but it is also largely balanced by the advection within the HBL. The magnitude of the gradient of the explicitly estimated SFS turbulence stress tensor is two order of magnitude larger than that of the turbulence parameterization schemes. In general the parameterization schemes of WRF-ARW model underestimate the turbulence effects on the resolved scale within HBL.

keywords: SGS and SFS Turbulence, TKE budget, Mixing length scale, Hurricane Boundary Layer

Acknowledgements

Foremost, I would like to express my sincere gratitude to my advisor Prof. Yongsheng Chen for the continuous support of my Masters study and research, for his patience, motivation, enthusiasm, and immense knowledge. His guidance helped me in all the time of research and writing of this thesis.

Besides my advisor, I would like to thank my thesis committee members Prof. Gary Klaassen, Prof. Peter Taylor and Prof. Dong Liang for their kindness, encouragement and insightful comments.

My sincere thanks also goes to Dr. Steve Allen, Centre de calcul scientifique, Université de Sherbrooke for helping me in writing the Message Passing Interface (MPI) and Python programs for processing big data files.

I would like to thank my fellow group mates Richard Liang, Geoffry Bell, Joanne Kennell, Abdulla Mamun, Nan Miao, Dr. Zhang Li and Dr. Zhoungshi He for the stimulating discussions during the weekly group meetings. Also I thank my friend Sangay Bhutia for the intense knowledge sharing and discussions as well as I would really like to thank Abhay Rai for being a great help and support during my research study.

My special thanks to the Dr. Paul Delany, Head of Natural Science division, York University for providing the financial support in the form of Teaching Assistantship. Also, I would like to express my gratitudes to Ms. Heather Moore and Ms. Donna Hewison, Faculty of Graduate Studies (FGS), York University for their kind support and Ms. Marcia Gaynor (graduate student assistant, ESSE, York University) for helping me into the administrative processes towards completion of my degree.

Last but not the least, I would like to thank my family for being supportive during my studies.

Dedicated to my beloved Mama

Table Of Contents

List of Tables

List of Figures

1 Introduction

1.1 The impact of hurricanes on human life

Hurricanes are the most intense form of tropical cyclones and major natural hazards affecting millions of people every year. Hurricanes are associated with very strong horizontal winds, and flooding due to torrential rain and coastal storm surge. Over the years, hurricanes have been responsible for injuries and loss of life, damage to structures, damage to shipping and fishing facilities, erosion of beaches, loss of soil fertility from saline intrusion, land subsidence, contamination of domestic water supply and destruction of vegetation and livestock (Southern, 1979). Hurricane Katrina(2005) is often used to provide an example of significance of hurricane-associated damages. The extent of damage resulting from Hurricane Katrina, including the death of more that 1500 people and the displacement of 500,000 others and more than $100 billion in damage costs suggests that there might be a high prevalence of mental health problems among those exposed to Katrina (Rosenbaum, 2006). The economic impacts of hurricanes are even more severe for developing countries *viz.* Caribbean and neighboring countries. Furthermore, the societal impact of hurricanes increases with coastal development - as the coastal population increases, there is even more economic vulnerability (Emanuel, 2005). Besides their economic impacts, hurricanes have also been responsible for the loss of thousands of human lives every year (Southern, 1979). However, better infrastructure, along with advance warning and preparation can substantially reduce the loss in human life and civil infrastructure. Improvements in the forecasts of hurricane tracks and intensities is a major part of the solution to avoid such calamities and fatalities.

1.2 Hurricane forecast

Hurricane track forecasts have been dramatically improved in recent years due to advancements in scientific fields such as high speed computing, high-resolution numerical modeling and due to the availability of higher quality observations. However, much room is left for improvement in the prediction of hurricane intensity by these models, and in the structure of rainfall predictions. Hurricane intensity depends critically on wind, temperature and moisture patterns in the core of the storm and in the nearby environment. While errors in forecasting the hurricane tracks have decreased by roughly 50% since 1990, there is still much to be learned about improving hurricane intensity forecasts. The reason for this uneven progress in forecasting of hurricane tracks and intensities is straightforward: hurricane tracks are mainly determined by large-scale steering flows (tropical-easterlies and mid latitude westerlies) that are increasingly being better resolved by global NWP models, whereas in addition hurricane intensities are influenced by inner-core dynamics and smaller-scale processes (*Viz.* fluxes across the air-sea interface,boundary layer convection, moist convection and cloud microphysics) that are poorly resolved or parameterized by global and even regional models(Benjamin and Zhang, 2013).

Additionally, the processes that govern intensities are inherently more chaotic and less predictable than those that govern tracks. According to American Meteorological Society (AMS) "For the 5-year period 2001-2005, NHC intensity forecast errors are averaged at 10 knots (5 ms^{-1}) for the 24-hours forecast and 14 knots ($7ms^{-1}$) for the 48-hour forecast" (AMS-Council-March, 2007). In contrast to the improvements for track, the mean intensity forecast errors have not changed significantly during the past 30 years Fig. 1.2. Accurate predictions of hurricane intensities are strenuous tasks because of the chaotic nature of atmosphere, insufficient observations and inherent deficiencies in the numerical models.

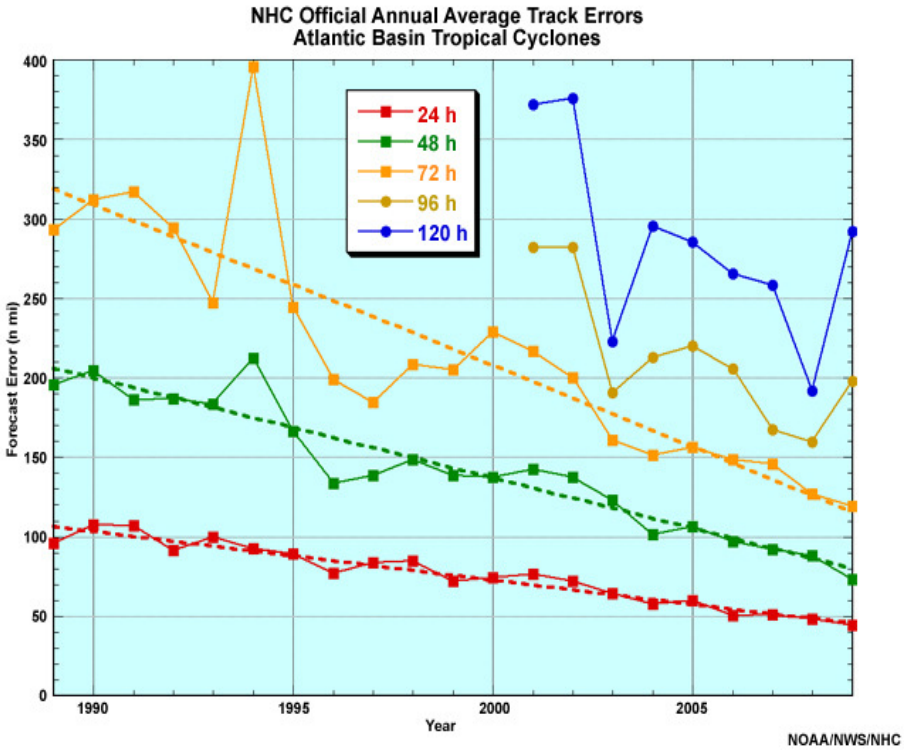

(a) Hurricane Track Error

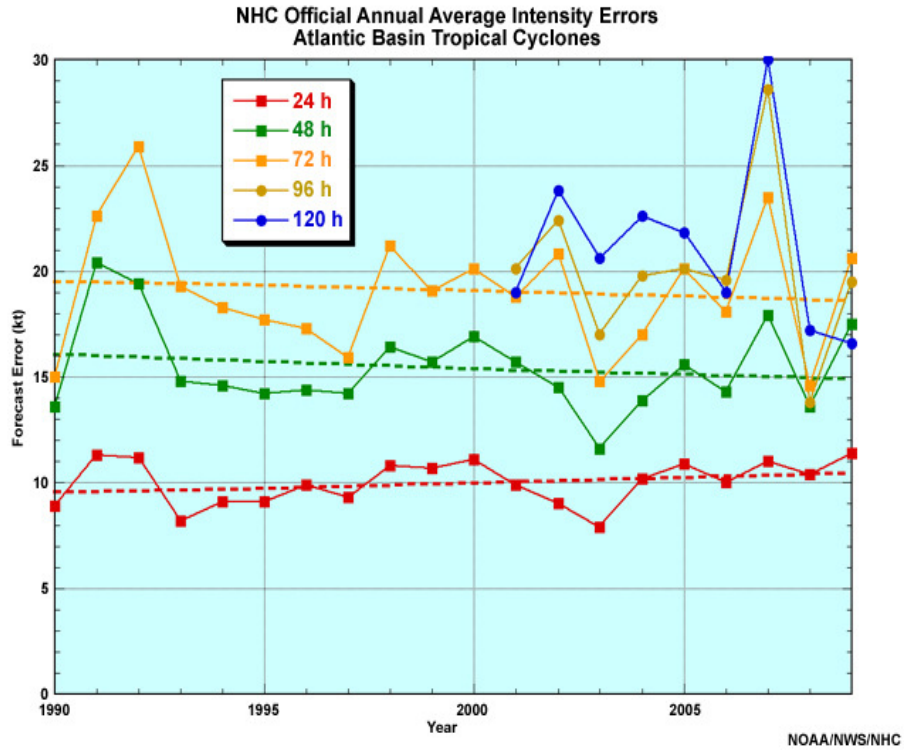

(b) Hurricane Intensity Error

Figure 1.2.1: NHC- Hurricane track and intensity forecasting error. *Courtesy: COMET Programm, UCAR*

1.3 Hurricane Boundary Layer

As noted by many previous studies (Vickery et al., 2009; Schroeder et al., 2009), wind characteristics in the Hurricane Boundary Layer (HBL) are appreciably different from wind characteristics in the standard ABL. The Atmospheric Boundary Layer (ABL) is the region of atmosphere near the surface where the influence of the surface is felt through turbulent exchange of momentum, moisture and enthalpy. A hurricane interacts with the ocean through HBL processes, obtaining heat and moisture, and transferring momentum to the ocean in the form of currents and waves. Studies focusing on the turbulent characteristics in the HBL indicated that the turbulence in hurricane winds is spatially better correlated and the turbulent kinetic energy is concentrated at frequencies lower than are found in the standard ABL (Li, 2012). These studies substantiated the need for a thorough understanding of the turbulent characteristics of the HBL, focusing on their differences from the turbulent wind characteristics of the standard ABL. Ample observations across the HBL are essential for interpreting physical, dynamical and thermal-dynamical processes, and hence for the development of models with realistic capabilities for forecasting or simulating hurricanes (Zhang, 2007). Turbulent mixing is the primary mechanism for the vertical transport of energy, moisture, and momentum in the boundary layer, yet it is a process that must be parameterized in numerical models due to constraints in resolution inherent in current models. These turbulent exchange processes are believed to be one of the controlling factors of hurricane intensity; but these processes are difficult to measure and characterize (Emanuel, 1997; Montgomery et al., 2009; Bryan and Rotunno, 2009a). Therefore, a thorough understanding and knowledge of these turbulent processes embedded within the HBL has become an integral part of hurricane research. There are several different strategies related to HBL research, as explained in the following sections.

1.4 Observational Studies

Turbulence within the HBL plays an important role in both air-surface exchange and in the destruction caused by storms at landfall. The HBL has been until now the least well-observed part of the storm due to a lack of in-situ measurements and because it is an extremely difficult environment for aircraft reconnaissance operations and surface based instrumentation to obtain direct measurements of the boundary layer structure due to safety requirements. Although endeavours of taking direct measurements of turbulence variables within the HBL had been made in the early 1970's, as described by Tuleya and Kurihara (1978), direct measurements of 3D turbulence within hurricanes are rare, because standard instrumentation is not designed to function in extreme winds and rain. Very recently the invention of research aircraft which operate safely at a sufficiently low altitude, like the ones used in the Coupled Boundary Layer Air-Sea Transfer (CBLAST) (Black et al., 2007; Zhang, 2010) field experiments, make it possible to take direct measurements of turbulent variables, like wind velocity variances and turbulent momentum fluxes within the HBL. The average turbulence horizontal mixing length near a hurricane inner-core is approximately 750m, corresponding to a mean wind speed of 52 ms^{-1} and at altitude $\approx$ 450m as shown in Fig. 1.4.1.

The other presently available technique for analyzing HBL turbulence is remote sensing. As described by Lorsolo et al. (2010), remote sensing techniques are able to reveal a crude structure of the HBL turbulence kinetic energy. Two-Dimensional profiles of Turbulence Kinetic Energy (TKE) were constructed, and revealed that the strongest turbulence was generally located in convective boundary layer with values of $5 - 10 m^2 s^{-2}$ in the lowest levels, in particular, in the eyewall, the magnitude of TKE often exceeds $15 m^2 s^{-2}$. Figure. 1.4.2a shows the interpolated ELDORA radar reflectivity in Hurricane Rita (2005) boundary layer which shows the presence of small scale eddies of the size of a few kilometers. Also the flight measurement on 500-meter height for Hurricane Hugo(2005) shows significant irregularity in wind structure which underlines the presence of turbulence in hurricane boundary layer (Fig. 1.4.2b). A correlation analysis of RADAR data showed that the strongest turbulence was generally associated with strong horizontal shear of vertical and radial wind components in the eyewall and strong vertical shear of horizontal

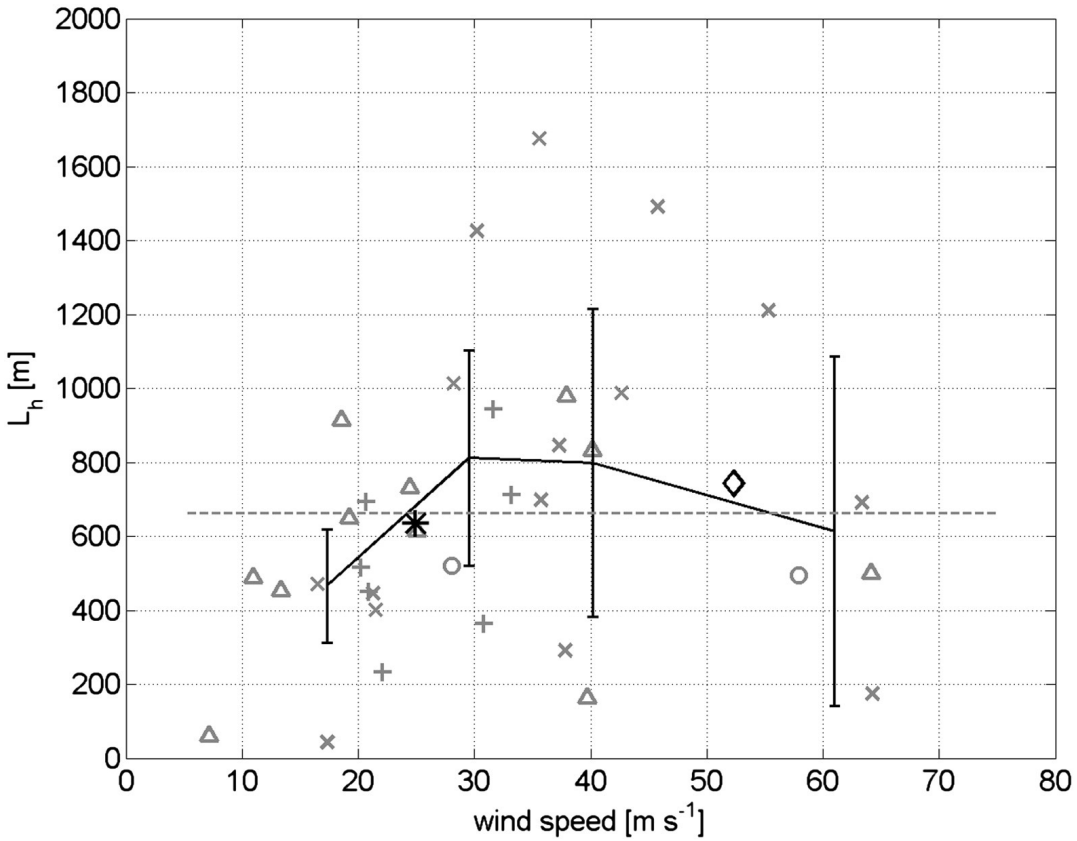

Figure 1.4.1: Horizontal mixing length l_h as a function of mean wind speed at flight level for all flux runs in Hurricane Allen (Δ), David ($\star$), Hugo (o), and Frances ($+$). (Zhang and Montgomery, 2012)

wind in the boundary layer. In addition to studies based on direct observations over water, measurements taken over land are also used to analyze turbulence characteristics within the HBL. Yu et al. (2008) estimated the wind spectra, cospectra and integral turbulence length scales of tropical cyclones and hurricanes using the surface wind data collected by the Florida Coastal Monitoring Program (FCMP). Their study showed that the turbulent energy at lower frequencies is considerably higher in hurricane-strength winds than those in non hurricane-strength winds. The integral length scale value estimated using 1-h averaged average winds is about 450m for category-2 hurricanes.

In recent years researchers are able to make unprecedented measurements of HBL wind velocities and other meteorological variables using newly developed GPS dropwindsonde techniques (Hock and Franklin, 1999). Li (2012) characterized the turbulence properties and estimated the integral length scales $\approx 300 - 450m$ at 700m height using GPS dropwindsonde measurements. These results suggests that both the velocity and height scales used in the turbulence diffusivity formulation of current generation hurricane

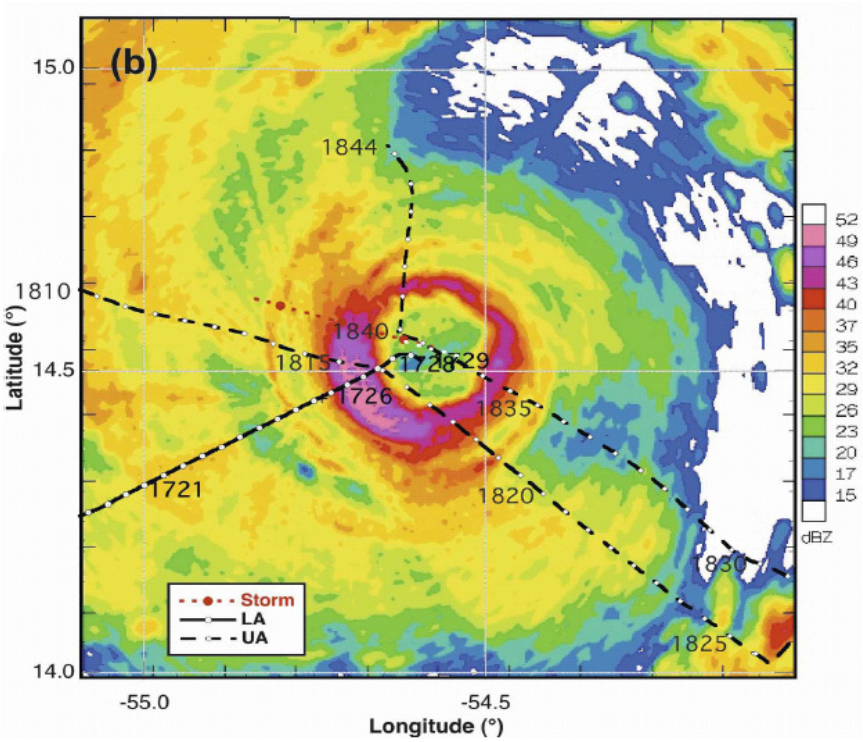

(a) ELDORA Radar Reflectivity Hurricane Hugo(2005),(*courtesy:COMET program UCAR*)

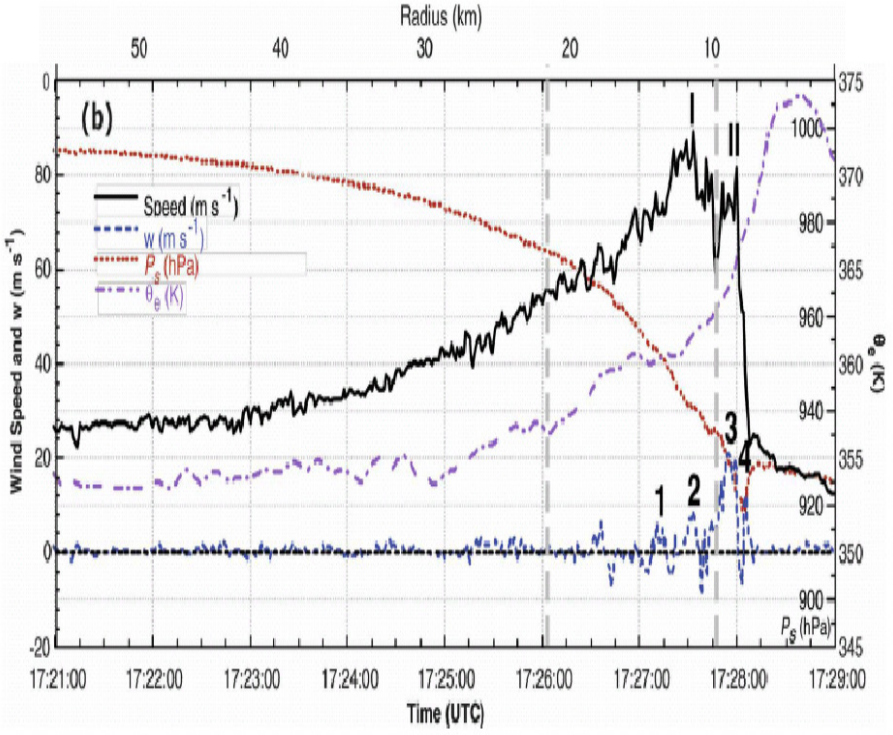

(b) Aircraft observation of Hurricane Rita(2005) at height 500m (Marks and Houze, 1987)

Figure 1.4.2: Turbulence structure from observation

forecasting models should be revised to take into consideration the special turbulence characteristics in the HBL. An integral length scale which is a measure of the diffusion of large-scale energetic eddies into smaller-scale eddies is widely used to model the turbulence characteristics within the HBL. An appropriate estimation of the eddy diffusivity or the integral length scale is very crucial in order to achieve better accuracy in hurricane intensity forecasts. Most of the observational studies/techniques show that the estimated integral length scale lies in the range between $\approx 300m$ to 700m below the altitude of 600m within HBL, and it increases with height from the surface upto $\approx 1.7km$ within the HBL (Zhang and Montgomery, 2012; Yu et al., 2008).

Despite all of this progress, comprehensive observations of the HBL have been especially hard to obtain, in particular observations of the small scale turbulent structures. Lack of data drives modelers to use boundary layer parameterization schemes that have mainly been developed for lower wind speed conditions. Modelers have typically extended the boundary layer parameterization schemes far beyond their validated regimes, and little detailed analyses of full-physics models results within the boundary layer have been carried out. However, the observed turbulence characteristics and the estimated integral length scale values have certainly improved our understanding and knowledge about complex turbulence processes within HBL. One objective of this current study is to use these limited observations/estimations to validate the current boundary layer parameterization schemes.

1.5 Modeling Studies of the Hurricane Boundary Layer

Understanding the very complex physical processes which drive enigmatic atmospheric phenomena like hurricanes has been of much interest among researchers for many years. Early theoretical studies of tropical cyclones (TC) focused almost exclusively on the dynamics of the moist convection and the kinetic energy of tropical cyclones (Yanai, 1964). A steady-state axisymmetric vortex model proposed by Ooyama (1969) has been considered as a stepping stone for TC modelling because it was the first model to take into account the effects of cumulus convection and boundary layer processes in the numerical simulations of TCs.

Hurricane intensity is dependent on many conditions *viz.* the larger-scale kinematic and thermodynamic environment, inner-core processes, and the cloud microphysics. Assumptions about boundary layer processes are particularly important to models attempting to simulate small-scale convection to mesoscale processes. The kinetic energy of the large-scale atmospheric circulations cascades down to mesoscale and smaller scale eddies through shear instability. The large-scale flow associated with the mechanisms of air-sea exchange across the boundary layer necessarily requires such processes in numerical models to be parameterized (Zhang, 2007). Simulating the influence of these small scale processes (*e.g.* turbulence, air-sea interactive processes etc.) likely requires running a numerical weather prediction (NWP) model at grid scales of $\Delta x << 1km$ so that the fine-scale structures of the storm are resolved and a turbulence parameterization scheme is no longer necessary (Yau et al., 2004). However, running operational NWP models for grid sizes where Δx is much smaller than 1km is still not a practical solution as it requires a lot of computational power. Hence an effective and accurate parameterization scheme of these sub-grid scale processes is important in order to improve forecasting skills of numerical models with grid size $\approx 1km$.

A recent study by Rotunno et al. (2009) revealed the importance of explicitly resolving the turbulence within the HBL. They found that the explicitly resolved turbulence weakens the radial gradient of angular momentum and entropy, which prevents the hurricane intensity from increasing. As argued by Rotunno et al. (2009), the simulated tropical cyclone is sensitive to the turbulence intensity in the HBL, which is, unfortunately, the

most uncertain part of a numerical simulation. By conducting a sensitivity analysis of the turbulence stresses on different turbulence parametrization schemes, this study will indicate that it is critical to find an appropriate boundary layer turbulence model.

Due to the importance of the turbulence parameterization on tropical cyclone simulations, efforts are continuously being made to propose a more accurate and realistic turbulence model. One recent study of (Zhu, 2008) involved modelling turbulence transportation based on large eddies. Using the Large Eddy Simulation (LES) framework in the Weather Research and Forecasting (WRF) model, this study derived some coherent structures relating to large eddies within the HBL. The simulation results support the idea that large eddies exist in a mainly stable environment and that they can be represented by large scale organized up-drafts and down-drafts. Zhu (2008) found that the organized up-drafts and down-drafts, or large eddies, interact with the sea surface, which make the main vortex more intense than produced by the turbulence parameterization scheme. This finding illustrated the need to devise a new parameterization scheme taking into account the large eddy effect in a hurricane model with insufficient resolutions. Zhu (2008) proposed a conceptual model, using statistical distribution of organized up-drafts and down-drafts revealed by the LES, which can be potentially implemented in any widely-used numerical model. Another pioneer study using LES to simulate the hurricane wind is that of (Rotunno et al., 2009). It described a LES simulation of an idealized tropical cyclone in a favorable environment. They discovered that the large eddies began to be resolved only when the model grid size was below 100m. Resolved turbulence has a great impact on the simulated hurricane wind field and its intensity. It increases the simulated turbulence gust while decreasing the mean maximum wind. Furthermore, this simulation showed noticeable differences between the resolved and parameterized turbulence, and therefore called for a further study on the small scale turbulence characteristics of the hurricane wind.

1.6 Objective

A more accurate hurricane intensity forecast is essential for improving hurricane prediction. The key issue of a better intensity forecast is to resolve or represent turbulent flows in the inner core region of a hurricane using numerical models. However, current computational resources have limited most operational hurricanes models to horizontal grid sizes of $\Delta x \approx 1km$ or more. While numerical forecasts at such resolutions can begin to capture some fine-scale asymmetries in the inner core region, they are still far too coarse for direct computations of three-dimensional turbulence, so this turbulence must be considered as sub-grid scale (SGS) motions. Therefore, all effects of the SGS turbulence have to be parameterized. Therefore important features of the numerical solutions depend sensitively on poorly known empirical constants in the parameterization schemes. Errors will be introduced in simulations if the SGS processes or the interactions between the SGS processes and the resolved processes are unrealistic. The SGS parameterization is one of the bottlenecks of numerical forecasts, and improving parameterizations is a way to alleviate this problem. However developing physically robust parameterizations of SGS motions has been proved to be an extremely difficult task. A better understanding and thorough investigation of these abstruse dynamics processes and turbulent structure of hurricane boundary layer is imperative.

The main purpose of this research is to investigate the effect of the explicitly resolved and parameterized turbulence on hurricane intensity forecasts using the Advanced Research WRF (WRF-ARW) model. It is a first step toward improving SGS turbulence parameterization scheme. In order to understand the impact of parameterized turbulence on hurricane intensity, a real case hurricane Danielle (2010) has been simulated using WRF-ARW with resolutions larger than 1km. The sensitivity of parameterized turbulence on hurricane intensity was studied by varying the empirical Smagorinsky constant C_s (related to the horizontal mixing length l_h) and the horizontal grid resolution Δx. The properties and characteristics of the explicitly resolved turbulence will be diagnosed and compared to the parameterized turbulence by using the high-resolution data generated from the LES of the idealized hurricane. The goals of this dissertation are divided as follows:

- To investigate the impact of parameterized turbulence on hurricane intensity via numerical simulations of a real-case Hurricane Daniel(2010) using the WRF-ARW model.

- To understand the HBL turbulence characteristics using the LES data, including

  ➢ Comparisons of SGS turbulence stresses computed using parameterization schemes of WRF-ARW model, namely the 2D and 3D Smagorinsky schemes (2D/3D SMG) and the 1.5-order Turbulent Kinetic Energy (TKE) closure scheme using filtered data.

  ➢ Estimations of horizontal mixing length scales and eddy-diffusion coefficients.

  ➢ Analyses of the spectral characteristics of HBL turbulent flow, the spectra and cospectra of momentum and heat fluxes.

  ➢ Diagnosis of Turbulent Kinetic Energy (TKE) budget estimated using explicitly resolved SGS turbulence.

Chapter 2 presents the simulation results of Hurricane Danielle (2010) and the sensitivities of its intensity on the model grid size and the Smagorinsky constant C_s. Chapter 3 reviews the WRF-ARW LES results. Chapter 4 illustrates the spectral scale separation of the LES data and compares the gradient of turbulence stress tensors computed explicitly using the resolved turbulence and those computed from the turbulence parameterization schemes using the filtered scale winds. In Chapter 4.2, the vertical profiles of turbulence fluxes are presented. Spectral characteristics of turbulence within HBL are examined, and the turbulent kinetic energy budget estimated using the explicitly resolved turbulence within HBL. The conclusions and the future work are given in Chapter 5.

2

Real-Case Study

As discussed by Emanuel (1997), the hurricane eyewall is major source of turbulence and can be treated as a front. It has been assumed that there is a clear scale separation between the horizontal and vertical mixing, and the vertical turbulence mixing in ABL is typically dominant. This assumption may not be valid when horizontal grid spacing approaches 1km or less, and a fully three-dimensional subgrid scale turbulence closure should perhaps replace the parameterized mixing (Wyngaard, 2004). As discussed in Section 1.5, Bryan and Rotunno (2009b) showed that the hurricane intensity is more sensitive to the horizontal turbulence mixing length scale (l_h) than the vertical mixing length scale (l_v). They used an axisymmetric model, in which the intensity of radial diffusion (mixing) is directly proportional to l_h. They found that the radial gradients in scalars and velocities are reduced as l_h is increased, and weaker radial gradients are consistent with weaker intensity, following the thermal-wind relation; that is, weaker radial temperature gradients are consistent with weaker vertical wind shear (thus, weaker azimuthal velocity).

In this chapter we are testing this sensitivity by varying horizontal mixing length l_h for simulations of Hurricane Danielle(2010), a category-4 hurricane with the WRF-ARW model.

2.1 Turbulence representation in WRF-ARW model

In global to meso-scale models the effect of SGS turbulence is parameterized due to their coarse resolutions. Most turbulence parameterization schemes represent subgrid-scale motion using the turbulent eddy diffusion relationship. The horizontal eddy diffusivity in numerical models typically takes the form of

$$K_h = l_h^2 S_h, \tag{2.1}$$

where

K_h=horizontal eddy diffusivity,

l_h=horizontal mixing length scale

S_h=horizontal deformation. The vertical eddy diffusivity K_v can be defined similarly. The WRF-ARW model uses turbulence closure schemes to represent subgrid-scale effects. These schemes are based in part on turbulence theory and observations. The K_h and K_v can be evaluated on model coordinates (eta levels) as well as on physical (x,y,z) space using stress and deformation tensors.

In the WRF-ARW model, vertical mixing is generally handled by planetary boundary layer (PBL) schemes while the horizontal mixing is parameterized using 2D/3D Smagorinsky schemes. The 2D Smagorinsky scheme uses horizontal deformation to calculate horizontal eddy diffusivity K_h by formula given below:

$$K_h = C_s^2 l^2 [0.25(D_{11} - D_{22})^2 + \overline{D_{12}^2}^{xy}]^{1/2} \tag{2.2}$$

where,

C_s=Smagorinsky Constant(default value in WRF-ARW is 0.25),

K_h=horizontal eddy diffusivity,

D=horizontal deformation,

l=Δx=grid distance.

Comparing eq. 2.1 and 2.2, the horizontal mixing length scale l_h is represented as $C_s(\Delta x)^2$. We can vary the horizontal mixing length scale l_h by varying the value of C_s

or the grid size Δx. While the 3D Smagorinsky scheme is similar to the 2D Smagorinsky scheme but both vertical and horizontal diffusions are computed and they depend upon the horizontal and vertical deformation and stability.

2.2 Case-Study: Hurricane Danielle(2010)

Hurricane Danielle (2010) was a Category-4 hurricane. Danielle developed from a tropical wave on August 21. The tropical depression strengthened and quickly became a tropical storm eighteen hours after its formation on August 22, and it reached category-2 on August 24. Also on August 24, Hurricane Danielle(2010) weakened back to a category-1 hurricane, but it returned to category-2 strength on August 25. The weakening of a subtropical ridge over the central Atlantic region caused a reduction in the forward speed of the hurricane which resulted in a weakened wind shear which led to a gradual strengthening of the hurricane on August 26. As the rate of deepening increased, the Hurricane Danielle(2010) became a category-4 hurricane with peak winds of 135 miles per hour (217 km/h) on August 27. Danielle slowly weakened in response to increasing southwesterly shear ahead of a deep mid-to upper level trough moving offshore of the east coast of the United States, and finally dissipated on August 30 Fig. 2.2.1. The hurricane was the first in a rapid succession of eleven named storms, which ended in late September.

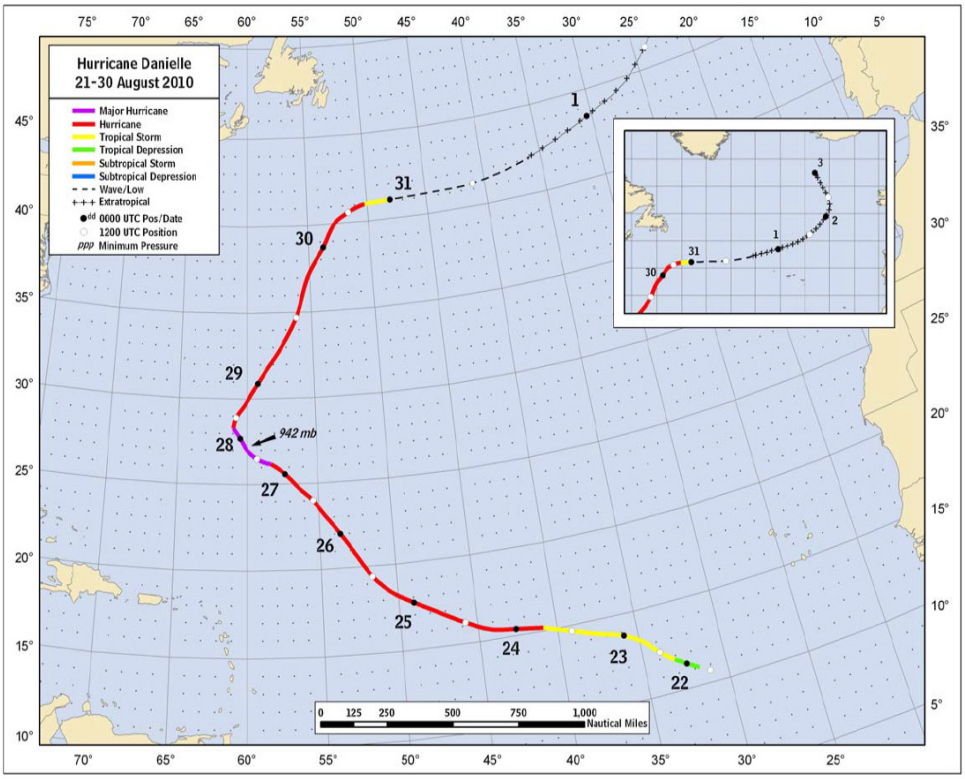

Figure 2.2.1: Best track positions for Hurricane Danielle, 21-30 August, 2010. Track during the extratropical stage is based on analyses from the NOAA Ocean Prediction Center. *Courtesy: National Hurricane Centre (NHC)*

2.2.1 Model Set-Up

For this study, we used WRF-ARW model version 3.3. The WRF model is a state-of-the-art, next-generation mesoscale numerical weather prediction system designed to serve both operational forecasting and atmospheric research needs (http://www.wrf-model.org). It is a nonhydrostatic model, with several available dynamic cores as well as many different choices for physical parameterizations suitable for a broad spectrum of applications across scales ranging from meters to thousands of kilometers. The dynamic cores in WRF include a fully mass- and scalar-conserving flux form mass coordinate version. The WRF-ARW model uses Arakawa-C grid staggering to compute the physical parameters. The time integration can be performed by using Runge-Kutta 2nd- and 3rd- order methods while the spatial discretization can be done by using the 2nd- to 6th- order advection options. The physics package includes microphysics, cumulus parameterization, planetary boundary layer (PBL), land surface models (LSM), and longwave and shortwave radiation (Skamarock et al., 2008).

The model was integrated for 120 hours (5 days) with storm-following nested domains. The outer most domain covers much of the northern part of the Atlantic Ocean Fig. 2.2.2. The model is run using the quadruply nested storm-following grids with resolutions of 36-12-4-1.33km and 35 vertical levels with 8 levels below 1km. The microphysics scheme being used is the WRF double-moment six-class scheme. The Kain-Fritsch convective scheme (Kain and Fritsch, 1990) is used for cumulus parameterization for the 36km and 12km domains. The Noah land-surface model and the Monin-Obukhov surface layer schemes are utilized to provide surface forcing. The Rapid Radiative Transfer Model Longwave radiation (RRTL) and Goddard short wave radiation schemes were used along with the YSU PBL scheme and a 2D Smagorinsky turbulence mixing scheme.

The model is initialized at 0000 UTC on the 25th August 2010 when Danielle was already a mature tropical storm. This time was chosen so as to avoid model spin up issues with cyclogenesis, and to be able to capture the peak intensity phase. National Centre for Atmospheric Research (NCAR) Ensemble Kalman Filter (EnKF) mean analysis data has been used for initial conditions. The model has been initialized with the same conditions

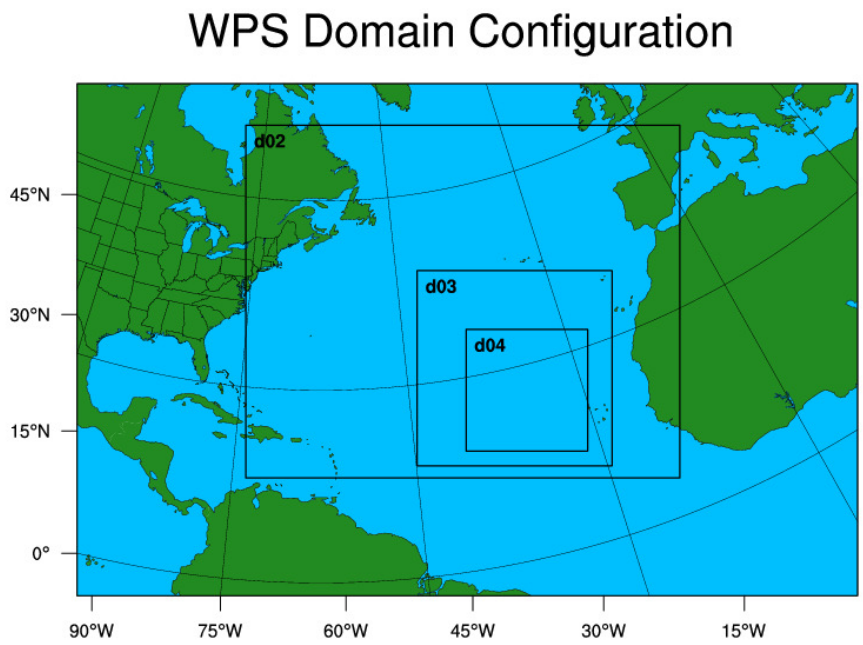

Figure 2.2.2: Domain set-up for simulating Hurricane Danielle(2010) with domain size D01=36km, D02=12km, D03=4km, D04=1.33km

but the resolution and the parameter C_s vary. The following section describes the effect of changing the resolution and C_s on the hurricane intensity and track forecast in detail.

2.3 Simulation Results of Hurricane Danielle(2010)

It has been seen that observed and a model-produced measures of intensity are not directly comparable (Kepert, 2006). The reason for this is that there are a lot of complex physical processes that cannot be resolved or possibly implemented into numerical models, yet are nevertheless of great influence in driving meso-scale phenomena. We have performed several sensitivity tests on Hurricane Danielle(2010) using the WRF-ARW model. The initial and boundary conditions are identical for all the simulations we performed, so any differences in intensities and structures are attributable to numerical model settings.

2.3.1 Sensitivity to Model Resolution

It is well known that simulated hurricane intensity is very sensitive to model resolution. Several studies have shown that numerically simulated intensity increases as the horizontal grid spacing decreases (Braun and Tao, 2000; Yau et al., 2004; Persing and Montgomery, 2003; Davis and Coauthors, 2008), at least for grid spacing $\triangle x \geq 1km$. We examined the sensitivity of hurricane intensity and track location on the model resolution by unvarying horizontal mixing length; specifically, we use C_s=0.25 and varied the model resolution from $\triangle x$=36km to $\triangle x$=1.33km by turning on the nested grids one by one.

As expected that the model simulations shows gradual increase in the hurricane intensity as the model resolution increases from 36km to 1.33km. As shown in Fig. 2.3.1 and 2.3.2, the hurricane becomes more intense as the resolution increases. It can be seen that when $\triangle x$=1.33km simulated Hurricane Danielle(2010) became a strong vortex with a maximum wind speed $W_{max} \simeq 60 ms^{-1}$ and the Minimum Sea Level Pressure (MSLP)$\simeq$930hPa. For Δx=36km Danielle(2010) became relatively weaker with a maximum wind speed $W_{max} \simeq 47 ms^{-1}$ and MSLP$\simeq$944hPa. For experiments with Δx=12, 4 & 1.33km, the intensification rate is higher than the observation or best-track data and the intensity reaches to the maximum values earlier. It is also interesting to notice that the MSLP's are nearly identical when Δx12km or higher, while the maximum wind speeds still exhibit large variations among different resolutions. The wind-pressure relationship will be studied in the near future. Figure. 2.3.3 shows Hurricane Danielle(2010) track forecast

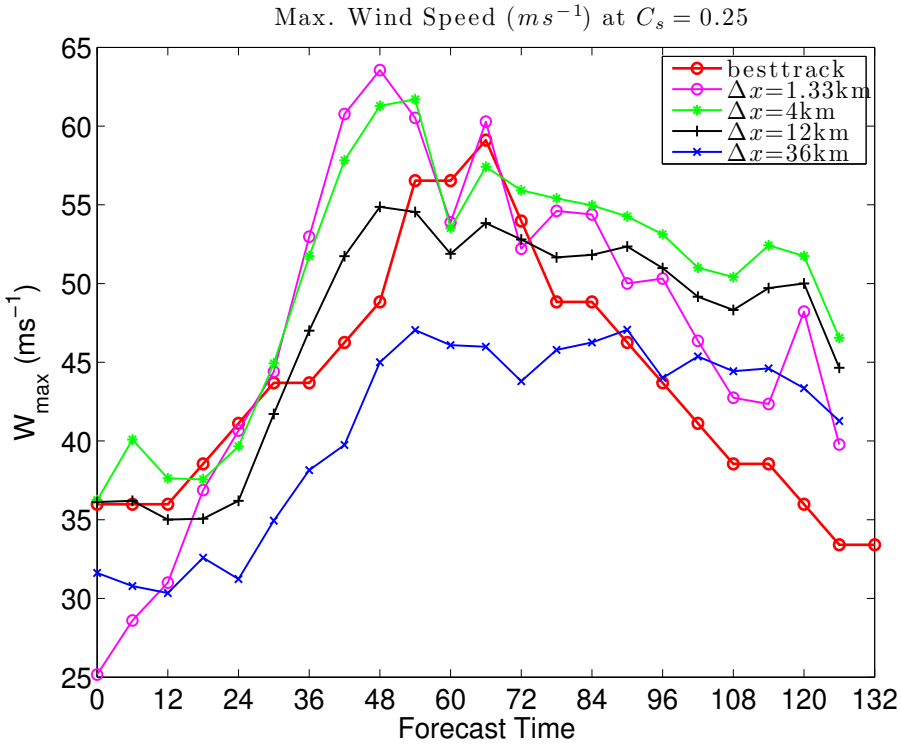

Figure 2.3.1: Hurricane Danielle(2010) Maximum wind speed $W_{max}(ms^{-1})$ for C_s=0.25

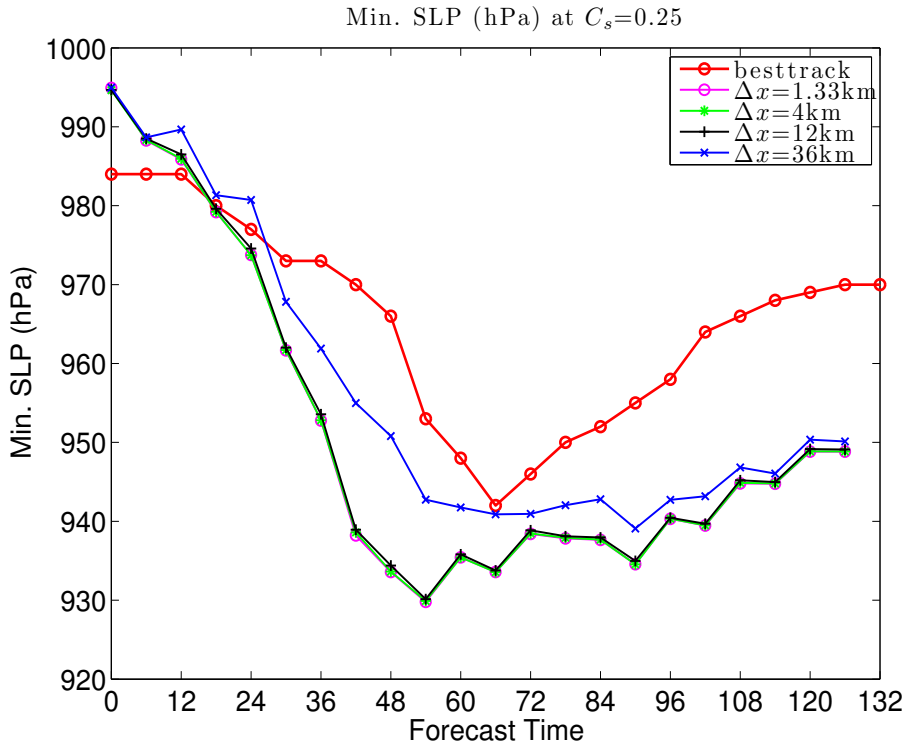

Figure 2.3.2: Hurricane Danielle(2010) Minimum Sea Level centre Pressure MSLP(hPa) for C_s=0.25

for all four experiments. The simulated track of Hurricane Danielle is not sensitive to the model resolution in the nested domain simulations. They took almost the same path - a

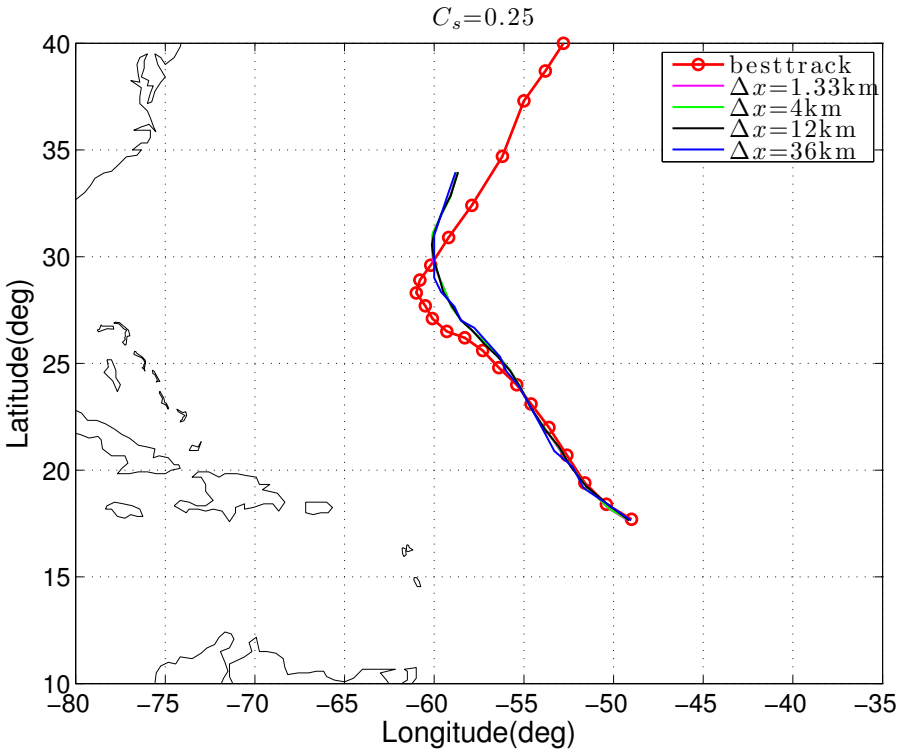

Figure 2.3.3: Hurricane Danielle(2010) simulated track for C_s=0.25

path which shows less curvature and is slower than the real/observed track.

2.3.2 Sensitivity to Horizontal Mixing Length Scale (l_h)

The WRF-ARW model uses turbulence closure schemes to represent subgrid-scale effects. These schemes are based in part on turbulence theory and observations. In the WRF-ARW 2D-Smagirnosky scheme, the horizontal diffusivity K_h is proportional to the horizontal mixing length l_h^2, which is in turn proportional to C_s. Here, we evaluate the sensitivity of the hurricane intensity and track to l_h by varying C_s. Firstly, we fix the resolution to $\triangle$x=1.33 km. The default value for C_s in WRF-ARW model is 0.25; but for our experiments we have changed the C_s value from 0.0 (no diffusion) to 1.0 (the maximum horizontal diffusion in our simulations).

Results in terms of W_{max} and MSLP are shown in Fig. 2.3.4 and 2.3.5. We can see that there is strong a sensitivity of W_{max} to C_s. The simulated hurricane is very intense with a maximum wind speed W_{max}=73ms^{-1} and MSLP=912hPa when C_s=0 and l_h=0. On contrary, if the maximum diffusion is allowed with the horizontal mixing length

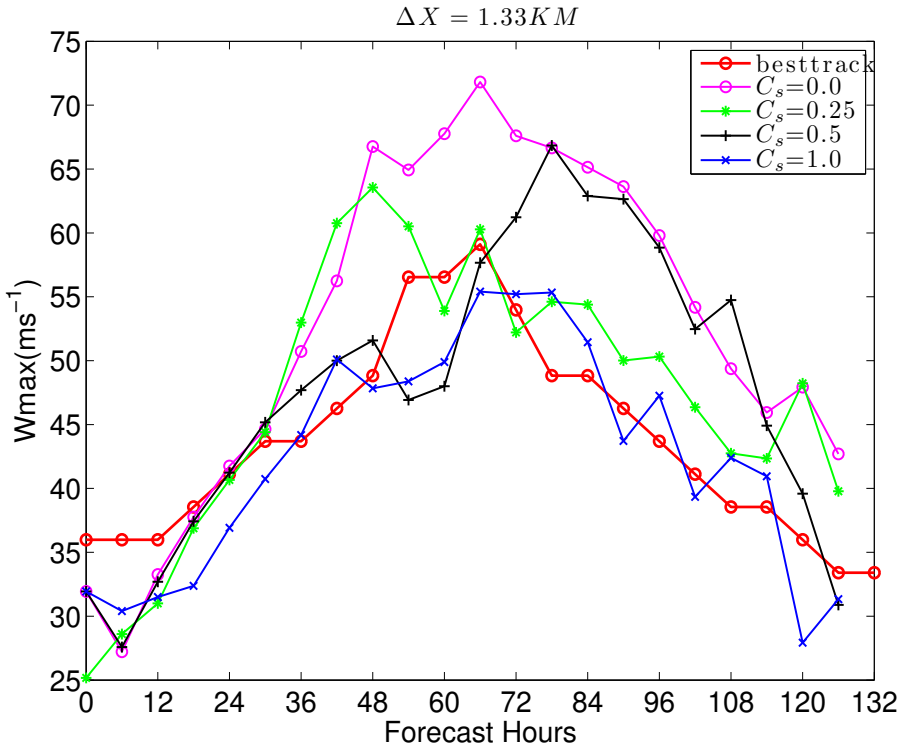

Figure 2.3.4: Hurricane Danielle(2010) Maximum wind speed $W_{max}(ms^{-1})$ for $\triangle$=1.33km, C_s varying from 0 to 1

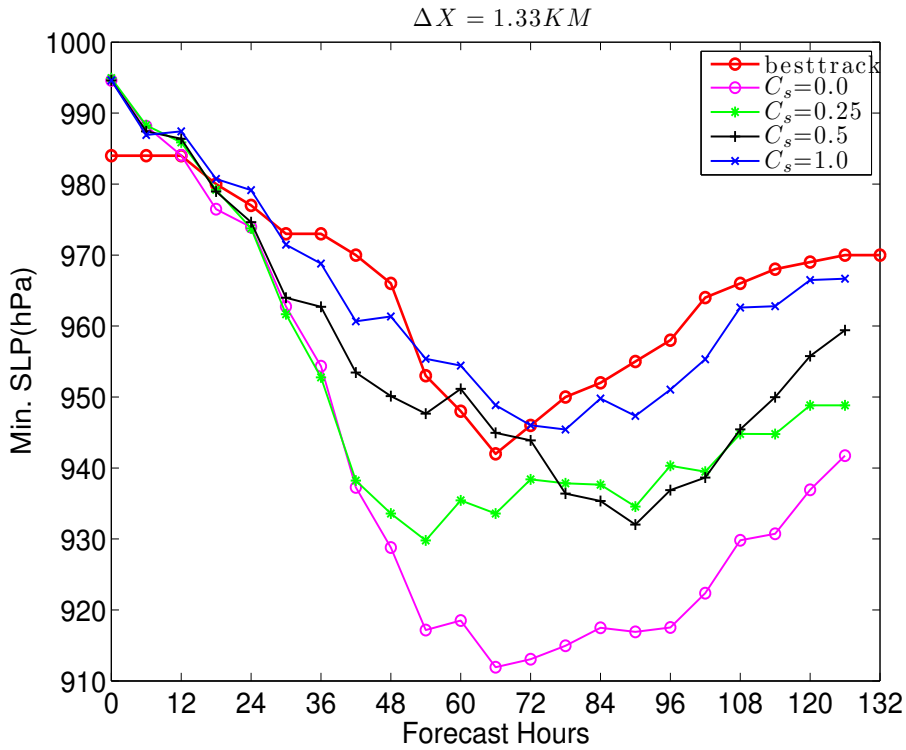

Figure 2.3.5: Hurricane Danielle(2010) MSLP (hPa) for $\triangle$x=1.33km, C_s varying from 0 to 1

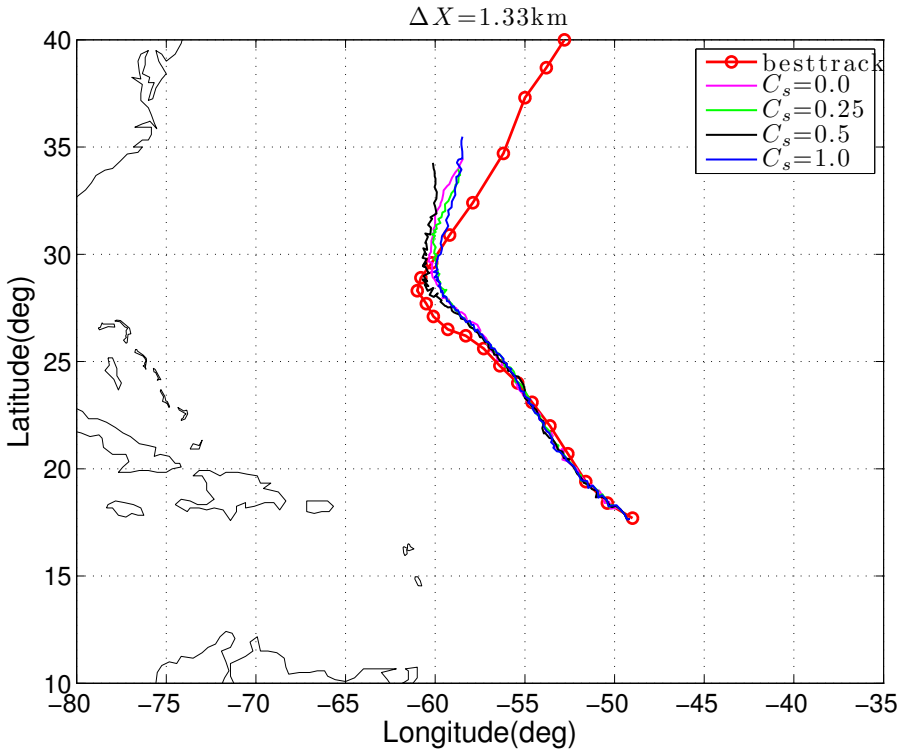

Figure 2.3.6: Hurricane Danielle(2010) simulated track for △x=1.33km, C_s varying from 0 to 1

l_h=1.33km by keeping C_s=1.0, the hurricane becomes much weaker with W_{max}=55ms^{-1} and MSLP=948hPa. Figure 2.3.6, shows the simulated hurricane tracks for varying l_h. Again, there is a little deviations among the simulated hurricane tracks, but they are also slower than the real track and the north-eastward turning is more gradual than the observed track.

Strictly speaking, varying both C_s and the model resolution △x will change the mixing length l_h. A set of experiments with combinations of different C_s and △x have been performed. The resulted maximum hurricane intensities and the forecast hours when the hurricane reaches its maximum intensity are summarized in the following tables.

	△x=1.33		△x=4km		△x=12km		△x=36km	
	W_{max}	hrs	W_{max}	hrs	W_{max}	hrs	W_{max}	hrs
C_s=0.00	71.81	67	70.22	72	63.96	69	50.56	75
C_s=0.25	64.83	68	63.49	68	54.87	51	47.66	66
C_s=0.50	70.53	89	67.32	86	62.90	87	55.41	87
C_s=1.00	60.00	71	63.00	72	58.32	75	53.11	75

Table 2.1: The maximum wind speed (W_{max}, ms^{-1}) and its forecast hours (hrs) from the simulations that use different values for C_s and Δx.

	△x=1.33		△x=4km		△x=12km		△x=36km	
	MSLP	hrs	MSLP	hrs	MSLP	hrs	MSLP	hrs
C_s=0.00	911.8	71	911.96	71	912.74	72	926.11	66
C_s=0.25	929.57	57	929.67	57	930.14	57	937.39	90
C_s=0.50	932.03	91	931.90	90	933	93	930.76	93
C_s=1.00	944.32	74	944.37	74	945.43	81	943.60	81

Table 2.2: The minimum Sea Level Pressure (MSLP,hPa) and its forecast hours (hrs) from the simulations that use different values for C_s and △x.

	△x=1.33		△x=4km		△x=12km		△x=36km	
	RMW	hrs	RMW	hrs	RMW	hrs	RMW	hrs
C_s=0.00	38.03	67	24.33	72	33.94	69	80.50	75
C_s=0.25	40.53	68	42.52	68	24	51	80.50	66
C_s=0.50	76.64	89	73.53	86	64.62	87	80.50	87
C_s=1.00	47.02	71	64.50	72	60	75	101.82	75

Table 2.3: The radius of maximum winds (RMW, km) and its forecast hours (hrs) from the simulation that use different values for C_s and Δx.

We can see that increasing l_h generally generates weaker hurricanes and vice versa. The hurricane intensity shows bigger sensitivity to C_s when horizontal resolution Δx is small.

2.3.3 Dynamic Structure of Simulated Hurricane Danielle

According to axisymmetric model results (Emanuel, 1997; Rotunno and Bryan, 2012), as $l_h \rightarrow 0$, the flow becomes essentially inviscid. In WRF-ARW when $l_h \rightarrow 0$, the maximum velocity obtained is W_{max} =75ms^{-1} when grid size is △x=1.33km and W_{max} =45ms^{-1} when grid size is △x=36km. The $W_{max} = 75ms^{-1}$ obtained for △x=1.33 km has greatly exceeded the maximum value of the observed $W_{max} = 55ms^{-1}$. To understand this further, we will examine the vertical structure of radial winds(V_r), azimuthal winds(V_t) and equivalent potential temperature(θ_e), as the radial gradient of all these physical parameters must be affected by change in l_h. Specifically, l_h increases horizontal mixing length for turbulent diffusion, which yields weaker radial gradient of physical parameters viz. momentum, winds,temperature etc. Figure. 2.3.7 and 2.3.8 shows the vertical structures of U wind component and V wind component on the south-north cross-section across the

hurricane centers in two experiments with $C_s = 0$ and $C_s = 1$, hence they are indicating tangential and radial wind respectively.

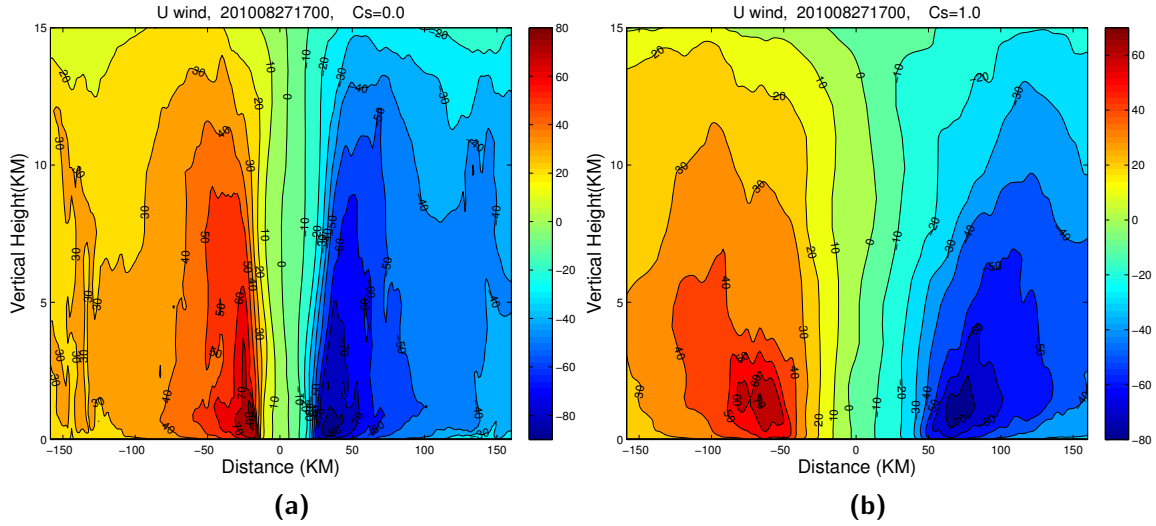

Figure 2.3.7: South-north cross-section of U-wind component (ms^{-1}) in simulated Hurricane Danielle(2010) valid at 17Z August 27, 2010 with $\Delta x = 1.33km$ and (a) $C_s = 0.0$ and (b) $C_s = 1.0$.

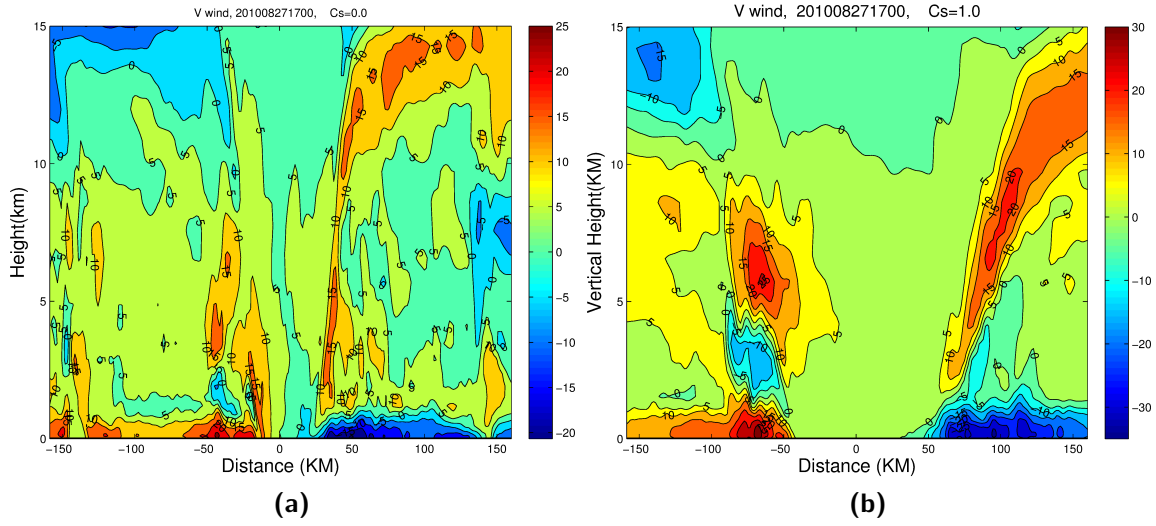

Figure 2.3.8: Same as Fig. 2.3.7 but for V-wind component

We can see that when $l_h \rightarrow 0$ the radial and tangential wind structures are more compact. There exists a sharp radial gradient of a tangential winds which extend higher when C_s=0. The strong inflow near the surface encounters the strong outflow inside the radius of the maximum wind (RMW), which indicates a maximum convergence near the eyewall and makes the hurricane more intense. On the other hand, when C_s=1(l_h=1.33km), the

large azimuthal winds do not extend very high and the RMW has also seen slanted outward. The radial inflow layer is taller, but the convergence near the eyewall is much weaker due to the elevated radial outflow layer. A stronger gradient in the equivalent potential temperature (Θ_e) near the eyewall resembles a front as discussed by Emanuel (1997). However diffusion is a frontolytic process; thus when l_h=1.33km (i.e. C_s=1.0) the horizontal diffusion becomes a significant factor reducing gradients in the equivalent potential temperature and winds which eventually weakens the hurricane intensity (Fig. 2.3.9).

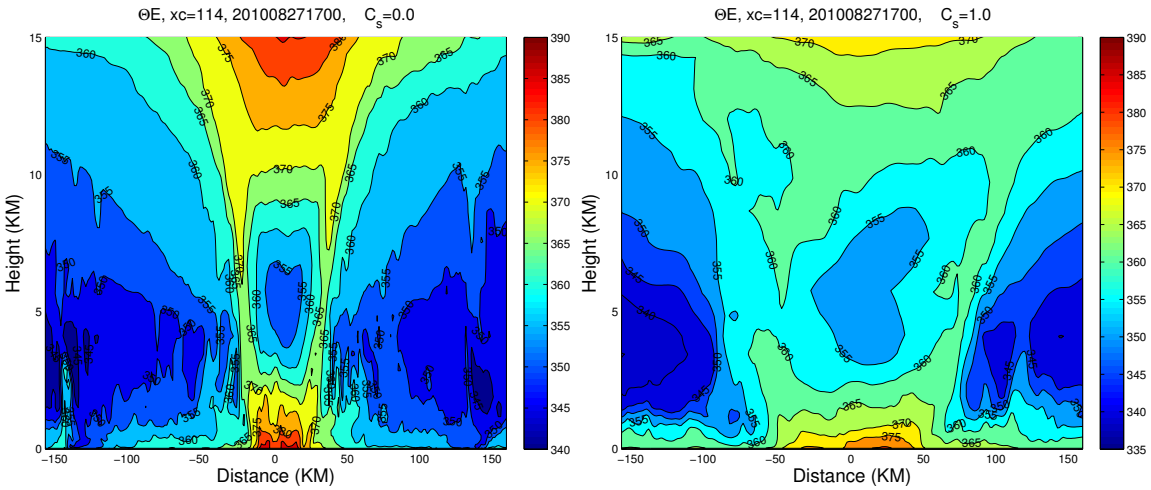

Figure 2.3.9: Same as Fig. 2.3.7 but for the equivalent potential temperature Θ_e

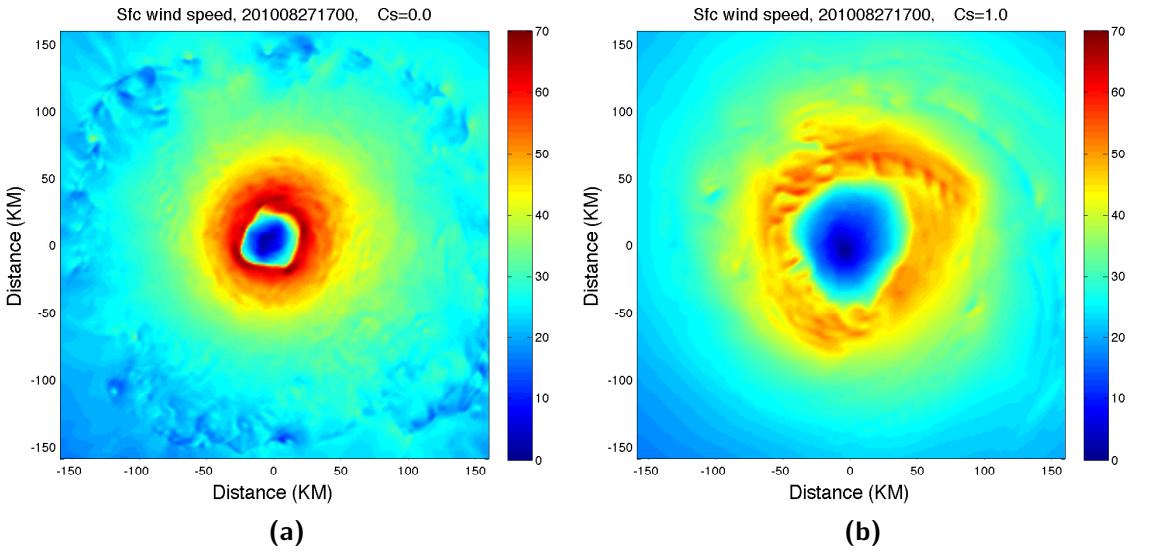

Figure 2.3.10: Same as Fig. 2.3.7 but for surface winds

Figure 2.3.10 compares the horizontal structures of surface winds at C_s=0.0 and C_s=1.0

when Hurricane Danielle(2010) briefly became a category 4 hurricane. At C_s=0, simulated Hurricane Danielle shows well developed eye with eyewall radius ≈20-25km surrounded by stronger and compact surface winds with W_{max} =70ms^{-1}. Whereas when C_s=1, simulated Hurricane Danielle(2010) shows comparatively weaker winds with (W_{max} =50ms^{-1}) around loosely formed eyewall with radius ≈40-45km.

One particularly interesting structure, a concentric eyewall appears in the simulation with C_s=0.0. The WRF-ARW simulated cloud water mixing ratio at ∼5km height shows the secondary concentric eyewall for hurricane Danielle at forecasting time T-54hrs Fig. 2.3.11. It is roughly at the same time the secondary eyewall was observed in real Hurricane Danielle(2010). The concentric eyewall and the eyewall replacement cycle are thought to change hurricane intensity rapidly. The vertical cross-section of tangential wind also shows the second wind maximum outside the primary maximum Fig. 2.3.11. Varying l_h not only changes the intensity but also alter hurricane structures significantly.

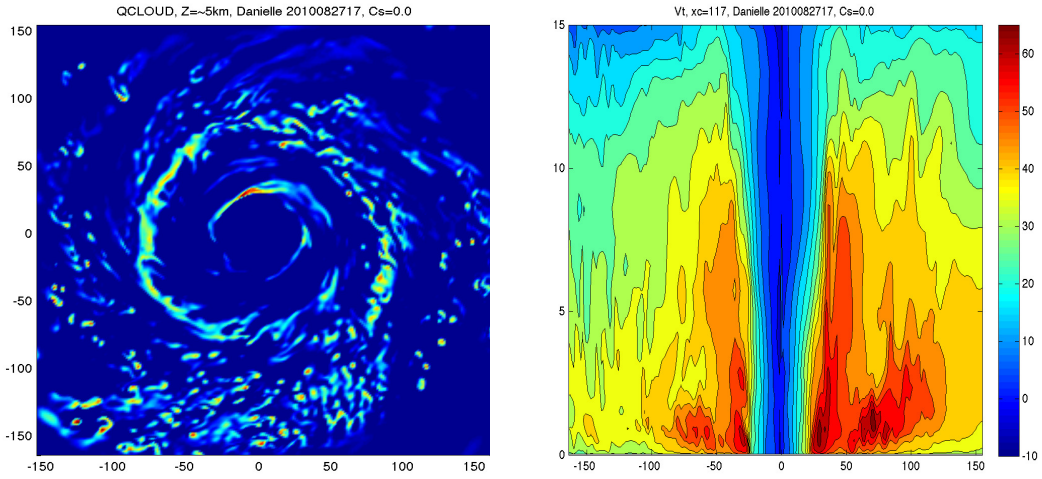

(a) **(b)**

Figure 2.3.11: (a) Cloud water mixing ratio at height ≈ 5km and (b) south-north cross section of tangential wind component when $C_s = 0$.

The numerical simulation of Hurricane Danielle(2010) showed that the intensity and track forecasts are sensitive to both the model resolution (Δx) and horizontal mixing length scale (l_h). If the model resolution is higher, WRF-ARW produces more intense Hurricane and vice versa, similarly when mixing length scale l_h decreases the intensity of the simulated hurricane increases and vice versa. The analysis of dynamic and inner-core

structure of simulated Hurricane Danielle(2010) is also very sensitive to the horizontal grid size(Δx) and mixing length scale l_h. The Hurricane Danielle(2010) also showed a concentric eyewall and an eyewall replacement cycle occurs when the horizontal diffusion is turned off in the numerical simulation. In summary, the intensity forecasting of the Hurricane Danielle(2010) has found to be very sensitive to boundary layer turbulence parameterization and model grid resolution.

3

Large Eddy Simulation

3.1 Introduction

In Chapter 2 we have investigated the sensitivity of horizontal mixing length scale on hurricane intensity and track forecast by simulation of Hurricane Danielle(2010) with the WRF-ARW operational forecasting model. We have seen that predictions of intensity forecasts for Hurricane Danielle(2010) are sensitive to both the model resolution and the turbulence horizontal mixing length. If the model resolution is higher, WRF-ARW produces more intense hurricanes and vice versa. Similarly when l_h decreases the intensity of the simulated hurricane increases. The analysis has also showed that the dynamic structure of the hurricane is also very sensitive to the grid size and mixing length scale. The simulated Hurricane Danielle(2010) has also showed that a concentric eyewall and eyewall replacement cycle occurs when the horizontal diffusion is turned off. A good turbulence parameterization scheme that can faithfully represent the actual turbulence effects in the NWP models is important to improve the accuracy of hurricane forecasts. Hence there is a need to understand the effects of turbulence in hurricanes.

As we have observed in Chapter 2, the hurricane intensity and its inner core structure are sensitive to the parameterized turbulence. Owing to the small-scale characteristics of the inner core, using high-resolution numerical models for intensity prediction is recommended. Most of the numerical simulations and predictions of hurricanes usually utilize a horizontal grid size Δ of 1km or larger. While numerical experiments at such resolution can begin to capture some fine-scale asymmetries in the inner core region, they are still far too

coarse for direct computation of three-dimensional turbulence (i.e. for large-eddy simulation or LES). All effects of turbulence have to be parameterized and therefore important features of the numerical solutions can depend sensitively on poorly known empirical constants. Recent work using an axisymmetric model by (Bryan and Rotunno, 2009a) finds a strong dependence of the maximum intensity of a hurricane on the assumed value for the horizontal mixing length. Rotunno et al. (2009) simulated an idealized hurricane using WRF-ARW in the LES framework with gradually increased resolutions from $\Delta = 1.67km$ to $\Delta = 62m$. In this and following chapters, we will analyze the turbulence properties in this LES dataset, and evaluate the turbulence parameterization schemes in the WRF model.

This chapter contains brief information of the LES followed by the overview of the WRF-LES results and characteristics of turbulence within HBL.

3.2 Large Eddy Simulation

Since the pioneering works of Smagorinsky (1963), Lilly (1966) and Deardorff (1970), LES has gradually become an important tool in atmospheric research. LES has successfully been employed in simulating a wide range of atmospheric conditions; from stable boundary layers to clear and cloudy convective boundary layers. As such, LES enables us to study processes and feedbacks in the ABL more accurately. Furthermore, as measurement/observation data is scarcely available, it can provide necessary 'synthetic' data to validate less advanced or lower resolution meteorological models (Stevens and Lenschow, 2001). However, as LES only resolves the most energetic scales of the turbulent flow, it relies partly on modelling the smallest scales of turbulence, introducing an uncertainty in the outcome of the LES model.

In terms of resolution, domain size and the resolved part of turbulence, LES models are classified in between direct numerical simulation (DNS) and Reynolds averaged (RANS) models. DNS completely resolves the turbulent flow by numerically integrating the Navier-Stokes equations, and therefore no turbulence closure (modelling of turbulence) is needed. This is illustrated in Fig. 3.2.1 where for DNS all turbulence, down to

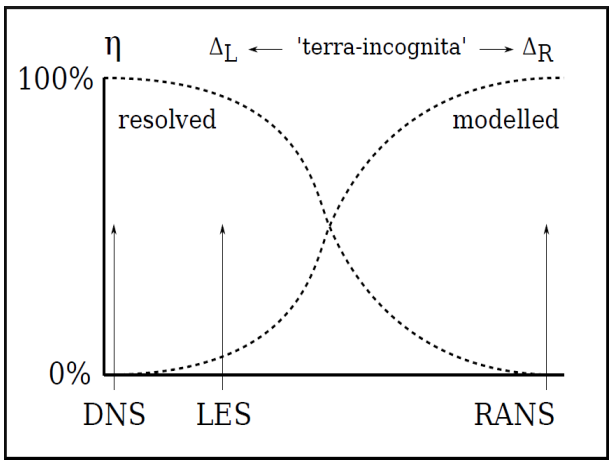

Figure 3.2.1: Percentage of resolved and modelled turbulence in DNS, LES and RANS models. Δ_L and Δ_R denote the typical grid spacing in LES and RANS models, η denotes the Kolmogorov length scale

the Kolmogorov length scale (η), is resolved. In contrast, RANS model uses the opposite philosophy, operating on scales such that no turbulence is resolved. Instead, all turbulence is modelled and only the resulting mean flow characteristics are described by the model. Both approaches have their pros and cons: By requiring no turbulence model, DNS remains physically close to reality. The downside of this approach is that all relevant turbulent scales (from the Kolmogorov to the integral length-scale) have to be resolved, requiring a very fine computational mesh. In DNS, the required number of grid cells $\mathcal{N}$ is by approximation proportional to the Reynolds number as $\mathcal{N} \propto Re^{9/4}$. With a typical Reynolds number of $\sim 10^8$ in a convective ABL, this results in $\mathcal{N} \approx 10^{18}$. In practice, this makes DNS impractical for simulations of the ABL. All operational forecasting models are RANS models (e.g. mesoscale models like MM5, WRF, RAMS), and so all turbulence is modeled. While this greatly reduces the required amount of computational power, it requires physical assumptions and *ad-hoc* tuning of model constants, resulting in a large uncertainty connected to the (partly) empirical closure of turbulence (Piomelli and Balaras, 2002).

LES was introduced as an intermediate solution. With a coarser grid resolution than DNS, the largest turbulent motions related to the production and transport of turbulence are resolved, which only the smaller scale turbulent motions related to dissipation require modelling. As a result, LES remains close to the true physical solutions of DNS, while the required computational power is reduced and simulations of typical atmospheric

cases become computationally amenable. However, this requires modelling of the sub-grid scale(SGS) turbulence. While the contribution of the SGS turbulence to the total turbulence is only small (10%, but often more in complex situations like a strong gradient near a solid surface), it plays an important role in the cascade of turbulent energy. Therefore, accurate SGS turbulence models are needed in LES.

3.2.1 Governing Equations

The development in both space and time of a turbulent flow is mathematically described by the Navier-Stokes equations. The Navier-Stokes equations for an incompressible fluid

$$\frac{\partial U_i}{\partial t} = -\frac{\partial U_i U_j}{\partial x_j} - \frac{1}{\rho}\frac{\partial p}{\partial x_i} + \nu\frac{\partial^2 U_i}{\partial x_i^2} + \mathcal{X}_i \tag{3.1}$$

form the basis for LES of the ABL, where U_i satisfy the continuity equations:

$$\frac{\partial U_i}{\partial x_i} = 0 \tag{3.2}$$

In Eq. (3.1) and (3.2), U_i is the flow velocity in the i^{th} three spatial directions (i.e., i=1 and 2 for the horizontal directions and i=3 for the vertical direction), $\mathcal{X}_i$ is the i^{th}-component of the body forces, whereas the major body forces are gravity and Coriolis forces), ρ is the air density, p is the pressure fluctuation, ν is the kinematic viscosity of the fluid, t is the time and x_i are the spatial coordinates.

The idea of LES is to compute the mean flow and the energy containing structures/eddies exactly while relying on the model to simulate the small scale structures. In LES, the scale separation and filtering are important in order to separate the mean flow into resolved and unresolved scales. The filtering operation extracts the large scale (vs small scale turbulence) information using the following relation

$$\overline{U}_i(x) = \int G(x, x')U_i(x')dx', \tag{3.3}$$

where G is the filter function. The full velocity can be expressed as

$$U_i = \overline{U}_i + u_i', \tag{3.4}$$

where $\overline{U}_i$ is called the resolved velocity and u_i' is the unresolved or sub-filter scale velocity. This decomposition allows the large scale quantities to be computed accurately on the coarse mesh which can have much larger mesh sizes than required by the DNS. Because the small scales are thought to be homogeneous and universal and are less affected by boundary conditions, the model can be simple and can theoretically be used in many types of flows. The most commonly used filters are the sharp Fourier cut-off filter, the Gaussian filter and the top hat filter. After applying the filter to the Navier-Stokes equations (Pope, 2000), the LES equation can be obtained (Pope, 2000). The incompressible LES equation can be expressed as follows

$$\frac{\partial \overline{U}_i}{\partial t} + \frac{\partial \overline{U}_i \overline{U}_j}{\partial x_j} = -\frac{1}{\rho}\frac{\partial \overline{P}}{\partial x_i} + \nu \frac{\partial^2}{\partial x_i x_j}\overline{U}_i - \frac{\partial \tau_{ij}}{\partial x_j}, \tag{3.5}$$

where the SGS stress tensor τ_{ij} is

$$\tau_{ij} = \overline{U_i U_j} - \overline{U}_i \overline{U}_j. \tag{3.6}$$

SGS terms are unknown term and have to be modeled in order to take into account the effects of the small scale turbulence. Eddy viscosity, similarity and mixed SGS modeling have been used and tested for decades. In these models, some studies assume that the filter is applied implicitly and some apply the filter explicitly to the SGS term.

The classical LES modeling can be categorized into three main groups: eddy viscosity models, similarity models and mixed models which combine the eddy viscosity and similarity models. The eddy viscosity models express the SGS stress tensor (τ_{ij}) in the following form:

$$\tau_{ij} = -2\nu_t \overline{S}_{ij} + \tau_{kk}\delta_{ij}, \tag{3.7}$$

where the $\tau_{kk}\delta_{ij}$ is the deviatoric part of the SGS stress tensor, and the strain rate tensor ($\overline{S}_{ij}$) is given by

$$\overline{S}_{ij} = \frac{1}{2}\left(\frac{\partial \overline{U}_i}{\partial x_j} + \frac{\partial \overline{U}_j}{\partial x_i}\right) \tag{3.8}$$

and ν_t is eddy viscosity which can be modelled in various ways. Most eddy viscosity models are based on equilibrium assumption of the viscous dissipation which removes the energy transferred from the large scales. The (Smagorinsky, 1963) is commonly used with the

following expression for the eddy viscosity.

$$\nu_t = (C_s\Delta)^2|\overline{S}|, \tag{3.9}$$

where C_s is the Smagorinsky constant, Δ is grid size, and $\overline{S} = \sqrt{(\overline{S}_{ij}\overline{S}_{ij})}$. The magnitude of the C_s varies for different flows. The advantage of the Smagorinsky model is that it can imitate the energy dissipation of the small scales very well, however it overestimates the dissipation near the wall and it is poorly correlated with actual SGS quantities computed from the DNS. The Smagorinsky model works well for flow which is homogeneous, statistically stable, isotropic in nature and whose mixing length-scale falls within Kolmogorov's spectra of inertial sub-range. The significant disadvantage of Smagorinsky model is the dependency of the coefficient C_s on the flow configuration.

3.3 WRF-LES set-up

The Weather Research and Forecasting model (WRF) is a numerical model designed for numerical weather prediction of the Earth's atmosphere. The WRF-ARW can be used in an LES framework. This approach has been proven useful to numerical weather prediction when experimenting with smaller than mesoscale phenomena. In the present study, the high-resolution data has been obtained from a series of numerical simulations of an idealized hurricane using WRF-ARW model with gradually increased resolution from Δx=1.67km to Δx=62m as reported in Rotunno et al. (2009). Here the high-resolution data has been further diagnosed and analyzed, in order to study the role of turbulence in the hurricane intensity forecasting.

The WRF model has been initialized by following a study of a vortex in an initially moist-neutral thermodynamic environment (Rotunno and Emanuel, 1987), where the advanced level experiments were carried to study an inner core structure of hurricane using LES. The LES framework in a hind-casting mode has been used by implementing a set of multiple two-way nested domains of WRF to explicitly simulate a spectrum of scales from large-scale background flows down to fine scale turbulent eddies. The model uses up to six telescopically nested grids centred on the hurricane vortex Fig. 3.3.1. The outermost

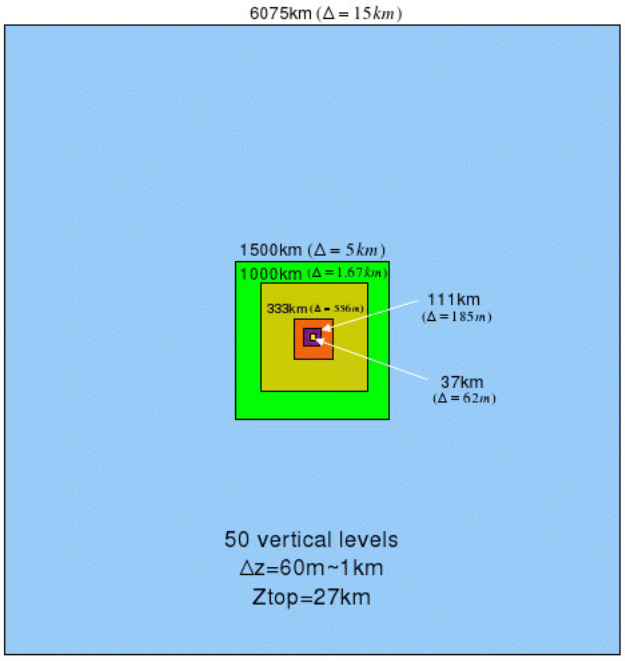

Figure 3.3.1: WRF-LES Domain Set-Up

domain has a resolution of △x=15km. Each subsequent nested domain has a grid spacing 1/3 of its parent domain. The parameters for all six domains are listed in table 3.1. There are 50 vertical levels with grid spacing stretching from 60m in the lowest level to 1.2km at the model top, with model top at 15hPa. No cumulus parametrization has been used on any of the domains. The moist processes are explicitly represented by the WRF Single-Moment 3-class scheme (WSM3). For the coarse-grid ($\triangle x$ >1km) domains, the Yonsei University planetary boundary layer (YU-PBL) scheme is used; while for domains with resolution $\triangle x$ <1km turbulence are parameterized using a grid-spacing dependent eddy viscosity based on a turbulence kinetic energy equation (TKE). The ratio of surface exchange coefficient for entropy and momentum Ce/Cd is effectively capped at 0.65 at high wind regime. To maintain a moist-neutral initial state, the radiation schemes are turned off, but a relaxation term is included in the thermodynamic equation to restore the initial temperature profile in a time scale of 36h.

The initial moist-neutral environmental sounding profile is computed following (Miglietta and Rotunno, 2005). The initial velocity field of an incipient tropical cyclone-like axisymmetric vortex with maximum lowest-level winds of $20ms^{-1}$, radius of maximum wind of 82.5 km, and radius of zero wind of 412.5 km following the analytical formula defined in (Rotunno and Emanuel, 1987). The vortex is evolving on a f-plane with f = 0.5x $10^{-4}s^{-1}$ over the ocean with a constant sea surface temperature 26.3^0C.

Domain	Domain Size(km^2)	Number of Grids	Resolution(m)	Time Step(s)
D1	6075x6075	406x406	15000	60
D2	1500x1500	301x301	5000	20
D3	1000x1000	601x601	1667	6.7
D4	333x333	601x601	556	2.2
D5	111x111	601x601	185	1.1
D6	37x37	601x601	62	0.37

Table 3.1: Parameters of all domains

3.3.1 WRF-LES Result

The experiment starts from the 3-domain integration. After the initial vortex develops into a mature and statistically steady hurricane, additional domains are telescopically nested to test the sensitivity of the numerical solution to resolution. The intensity of idealised hurricane in all the coarse domains except domain-6 became almost steady after 9 days of the simulation. The horizontal distribution of the 500-m wind fields obtained from the WRF-ARW LES has shown in Fig. 3.3.2. In domain-3, the region of strongest winds in the inner core is rather broad and V_{max} barely exceeds $60ms^{-1}$. The vortex contains a modest asymmetry but is generally axisymmetric. The vortex strengthens remarkably in domain 4 and 5, yet still retains its nearly axisymmetric character. It has seen that the maximum wind increases as the resolution increases from D3-D5.

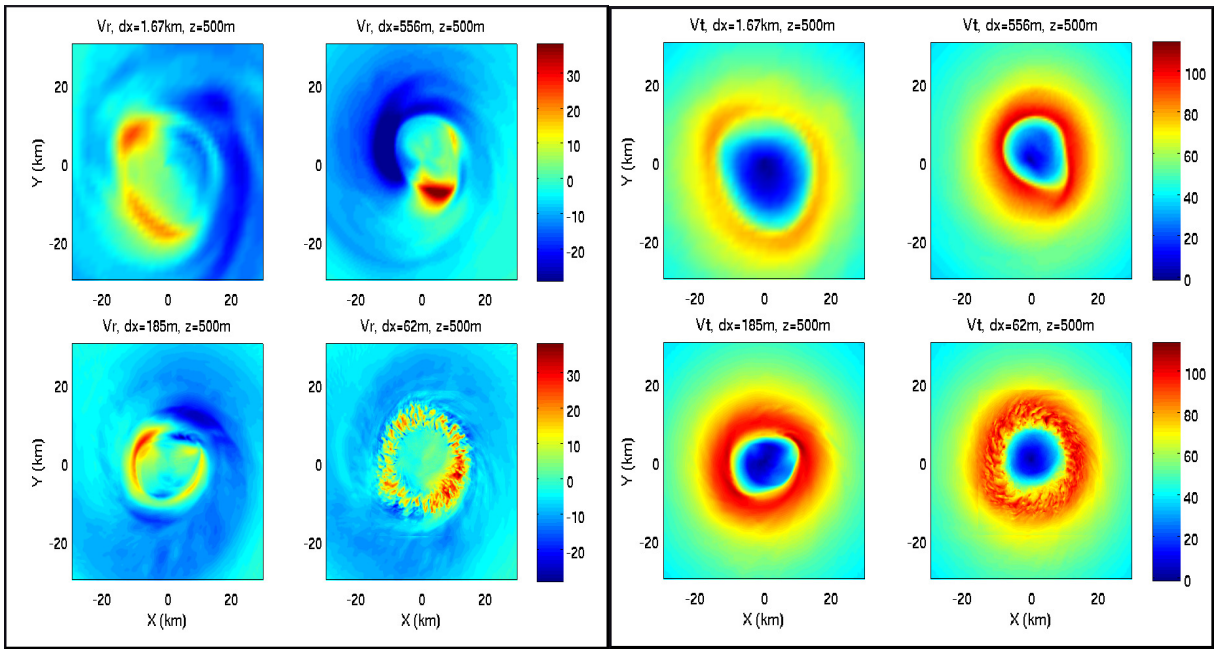

(a) Radial Winds **(b)** Azimuthal Winds

Figure 3.3.2: Winds for domain width $\Delta x = 1670M$,$\Delta x = 556M$,$\Delta x = 185M$ and $\Delta x = 62M$ respectively

At $\Delta x = 62m$ i.e. in domain-6, a distinct change occurs with the flow structure characterized by vigorous, small-scale eddies within the annulus of strong winds with maximum wind speed $\approx 122ms^{-1}$. The marked change in wind structure suggests a transition to randomly distributed, small-scale turbulent eddies when the grid-size is decreased from

185m to 62m. The significant increase in maximum wind variability for domain-6 is indicative of the short lifetime of these turbulent eddies. This is confirmed by a 1-minute average wind speed for 9.75 days, which almost completely removes the small-scale variations and reduces the maximum winds to $79 ms^{-1}$. Clearly, the LES of hurricane core strongly suggests that passing to a sub 100m grid produces a partially resolved turbulence in the inner core of idealized hurricane.

The large eddy simulation of the idealized hurricane shows the dependency of the hurricane intensity and inner core structure on the model resolution and resolved turbulent eddies (Bryan and Rotunno, 2009b). It is found that the model produces energetic turbulent eddies when the grid interval falls below approximately 100m. The results also suggest that it is necessary to properly model subgrid-scale turbulence, when the resolution is high, but not high enough to resolve all turbulent eddies. In short, the larger the turbulent diffusion, the weaker the intensity of the simulated vortex. This dependence underlines the quantitative importance of the internal turbulent diffusion in a tropical cyclone (about which little is known) for both high-resolution numerical simulations and real-time predictions of tropical-cyclone intensity.

3.4 Spectral characteristics of HBL

The major goal in the development of any NWP model is to maximize model efficiency, where efficiency is defined as the accuracy of the solution relative to the cost of numerical integration. Global forecast models and climate models generally reproduce the large-scale K_H^{-3} spectral characteristics i.e. characteristic of 2D turbulence, and transition to a $K_H^{-5/3}$ dependence in the mesoscale which is a characteristic of 3D turbulence (Laursen and Eliasen, 1989). Observations and theoretical studies appear to conclude that the turbulent flows in the HBL can be thought of as a superposition of coherent eddy pattern of velocity, vorticity and pressure spread over wide range of scales (Kaimal and Finnigan, 1994). These multiscale eddies interact constantly with the mean flow by exchanging energy and momentum. Different scales of turbulent motion must be isolated in order to understand the conversion of mean kinetic energy into turbulent kinetic energy in the large eddies, energy cascading and conversion to heat by viscosity (Stull, 1988). This could be achieved via spectra and cospectra of the turbulent variances and fluxes to determine the dominant contributing scales in the evolution of the mean flow. The study of spectra and cospectra can also reveal information about the overall boundary-layer structure and dynamics.

3.4.1 Kinetic Energy Spectra

The turbulence energy fluctuation may be viewed as a superposition of eddies, each characterized by a wavenumber $K = 2\pi/\lambda$, where λ is the wavelength. The total kinetic energy of the turbulent motion may, correspondingly, be regarded as a sum of contributions by each of the eddies of the flow. The function representing the dependence upon wavenumber of these energy contributions is defined as the energy spectrum of the turbulent motion.

In wind, larger or low-frequency eddies generate turbulent energy and smaller or high-frequency eddies dissipate it through eddy viscosity/diffusivity. This phenomenon is referred to as the energy cascade, which consists of three major spectral regions. In the

lower frequency range, energy is produced by buoyancy and shear. In the highest frequency range, kinetic energy is converted into internal energy (viscous dissipation). In the intermediate or inertial subrange, energy is neither produced nor dissipated if the flow is horizontally homogeneous and neutrally stratified (Kaimal et al., 1972).

Power spectral analysis of the winds are useful in determining temporal (in terms of the frequency) and spatial (in terms of the wavenumber (K) or wavelength (λ)) scales of the turbulence. The kinetic energy spectra have been computed on every model level using a 2D Discrete Cosine Transform (DCT2, Denis et al. (2002)). We first transform three velocity components (u, v, and w) into a 2D spectral space, then the kinetic energy spectra was computed in the 2D spectral space. The 1D spectra were obtained by averaging the 2D spectra according to their total wavenumbers.

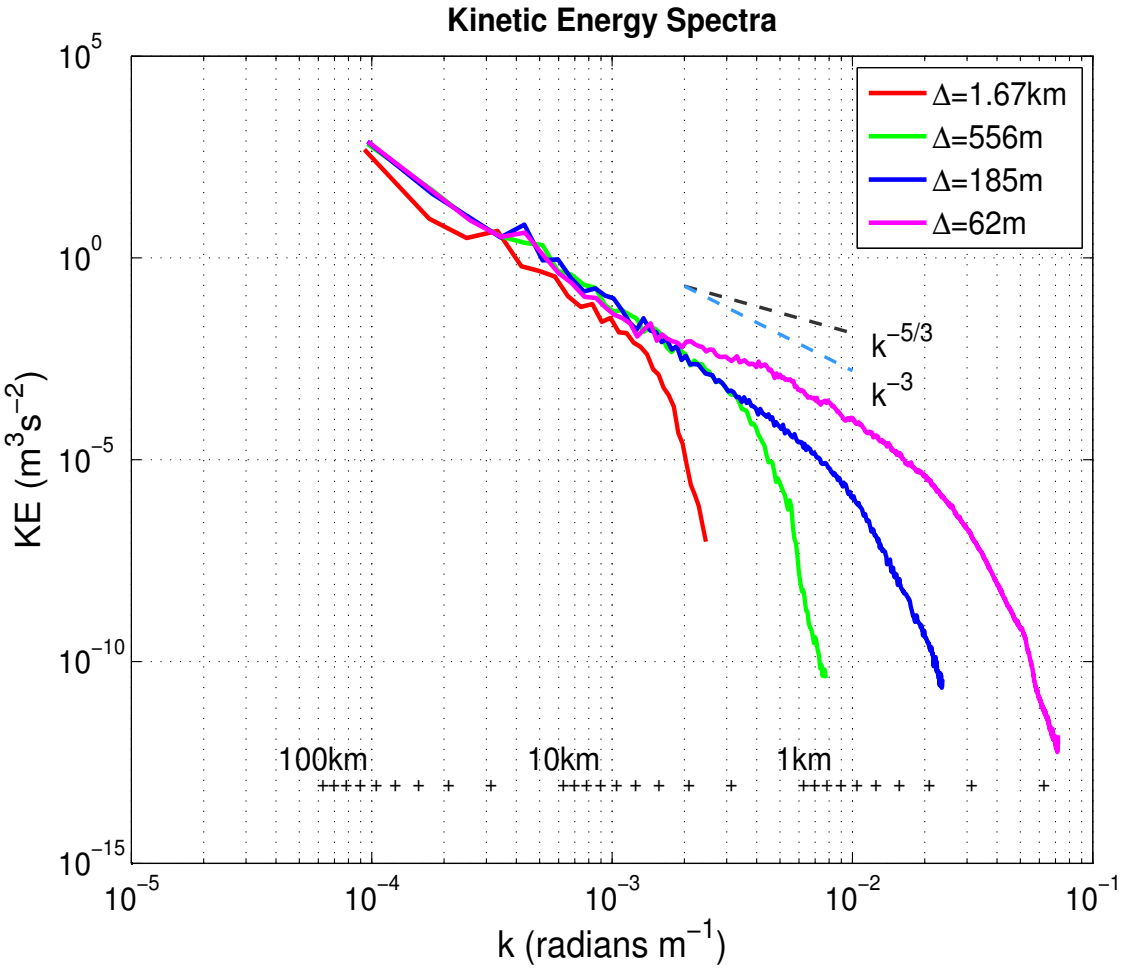

Figure 3.4.1: Kinetic energy spectra for all the domains at height Z=120m

Figure. 3.4.1, shows the kinetic energy spectra generated using the simulation data with the grid resolution of 1667m, 556m, 185m, and 62m respectively. The power spectra

begins to appear as a turbulent flow with Kolmogorov-Kraichnam scaling with constant slope of $K^{-5/3}$ at model resolution $\Delta x = 62m$. The domains with grid-size $\Delta x = 185m$ and $\Delta x = 556m$ have a shallower $K^{-5/3}$ slope which indicates a smaller spectral range under the inertial subrange. As well, a coarser resolution domain with grid size $\Delta x = 1.67km$ does not show any sign of an inertial subrange region. The LES kinetic energy spectrum has a kink at about a $\lambda = 3km$ wavelength which has been significantly under-estimated in the coarser resolution simulation with grid size $\Delta x = 1.67km$ and $\Delta x = 556m$ respectively.

The WRF-LES model have been able to resolve the large energetic turbulent eddies which are homogeneous, isotropic and statistically steady in nature if the model resolution is $\sim \Delta 62m$, but failed to capture an inertial subrange and turbulent eddies when the grid resolution is coarser $\sim \Delta x > 180m$. It can be inferred that the operational weather forecasting models with horizontal resolution $\sim \Delta x = 1.67km$ are not adequate for the subgrid scale models to be appropriate.

3.4.2 Spectral characteristics

All the physical fields computed by WRF-ARW model are multidimensional, and multidimensional transforms are most often used for their decomposition. An spectral decomposition approach such as DCT as described in Denis et al. (2002) has been typically employed to collapse results from a 3D or 2D transform to a single dimension by integrating the energy density over shells in the wavenumber space. In this study the cospectral has been computed for the finest domain with resolution $\triangle$x=62m.

The spectra of radial(S_{uu}), azimuthal S_{vv} and vertical S_{ww} winds are generated using WRF-LES data. Figure 3.4.2 shows the spectra of kinetic energy spectra from three wind components plotted as a function of wavenumber(K) approximately at height 100m above the surface; the spectra follow Kolmogorov's $K_H^{-5/3}$ universal law; conforming that the Monin-Obukov similarity theory works well for the wind velocity spectra in the hurricane boundary layer.

The region of turbulence energy spectra which comes under $K_H^{-5/3}$ slope follows the wavelengths range from ~500m-3000m. The spectra estimated using WRF-LES output also matches well with wind spectra obtained within HBL for hurricane Fabian(2003) and

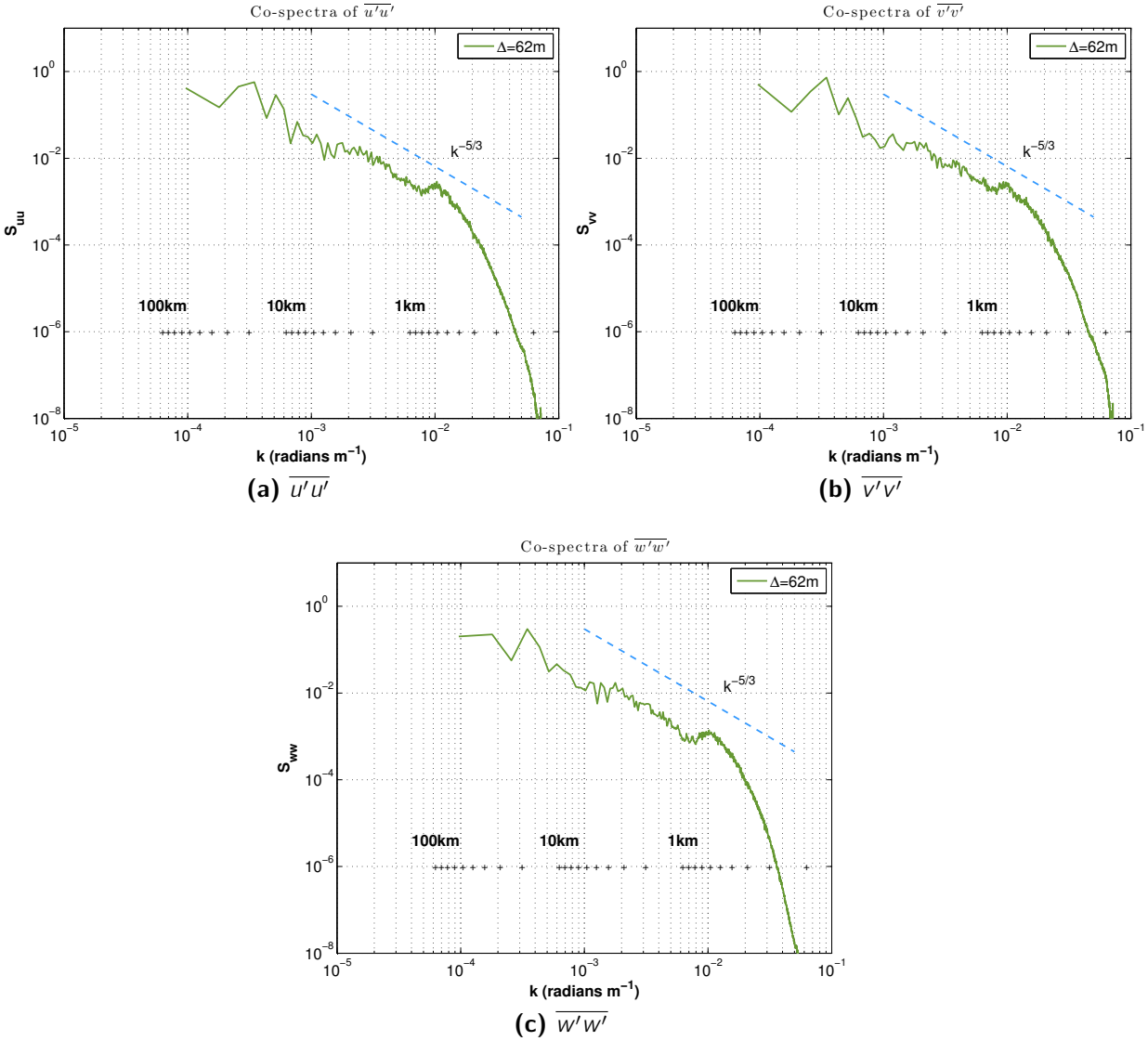

(a) $\overline{u'u'}$ **(b)** $\overline{v'v'}$ **(c)** $\overline{w'w'}$

Figure 3.4.2: Cospectra of $\overline{u'u'}$, $\overline{v'v'}$ and $\overline{w'w'}$ momentum fluxes (*unit:* m^2s^{-2}) follows $K_H^{-5/3}$ slope.

Isabel(2003) in the CBLAST experiment (Zhang, 2010). All three decomposed energy spectra of u,v and w follows Kolmogorov $K_H^{-5/3}$ law very well and shows a spectral energy peak almost in the same wavenumbers range for azimuthal and radial winds. The vertical winds (w) are showing the $K_H^{-5/3}$ spectral slope but slightly in the higher wavenumber range compared to the horizontal winds and consistent with the studies done by Rotunno et al. (2009) about the 3D turbulence nature of HBL. The vertical winds are slightly weaker in strength than the horizontal winds within the HBL and it shows the spectral peak at slightly higher wavenumber(K) compared to the horizontal winds.

Figure 3.4.3, shows WRF-LES generated cospectra for S_{uw} and S_{vw} momentum fluxes

which are showing almost the same peak wavelength of ∼900m. This indicates that the scale of the dominant eddies transporting momentum are present in inertial subrange region of the turbulent spectra with size ranging from few hundred meters to 3km. These dominant eddies are playing a crucial role in hurricane intensification by cascading turbulent energy downscale from the large eddies to small-scale eddies concluding in eventual eddy destruction through viscous dissipation. These dominant eddies need to be resolved correctly and parameterized accurately in operational NWP models for better hurricane intensity forecast.

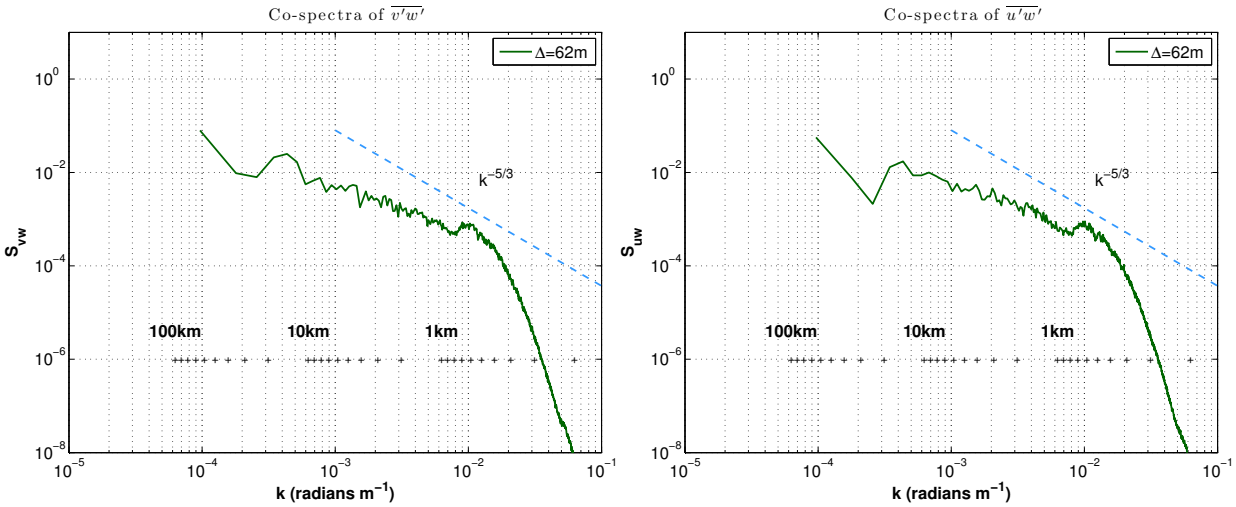

(a) $\overline{v'w'}$ **(b)** $\overline{u'w'}$

Figure 3.4.3: cospectra of $\overline{v'w'}$ and $\overline{u'w'}$ momentum fluxes (*unit:* m^2s^{-2}) follows $K_H^{-5/3}$ slope

Figure 3.4.4, shows the spectral behavior of vertical fluxes of potential temperature and humidity. Humidity and potential temperature spectra show almost similar shapes as those of the momentum flux spectra. The potential temperature and humidity flux spectra show the same broad range of energy containing eddies with nearly no sign of clear inertial subrange. This makes it difficult to identify the peak wavelength flux.

The inability of current operational forecasting models to capture the effects of turbulence through SGS turbulence parameterization schemes is believed to be a significant factor in the lack of accuracy of current hurricane intensity predictions. It is necessary therefore to review or modify current SGS turbulence parameterization schemes for use with coarser domains.

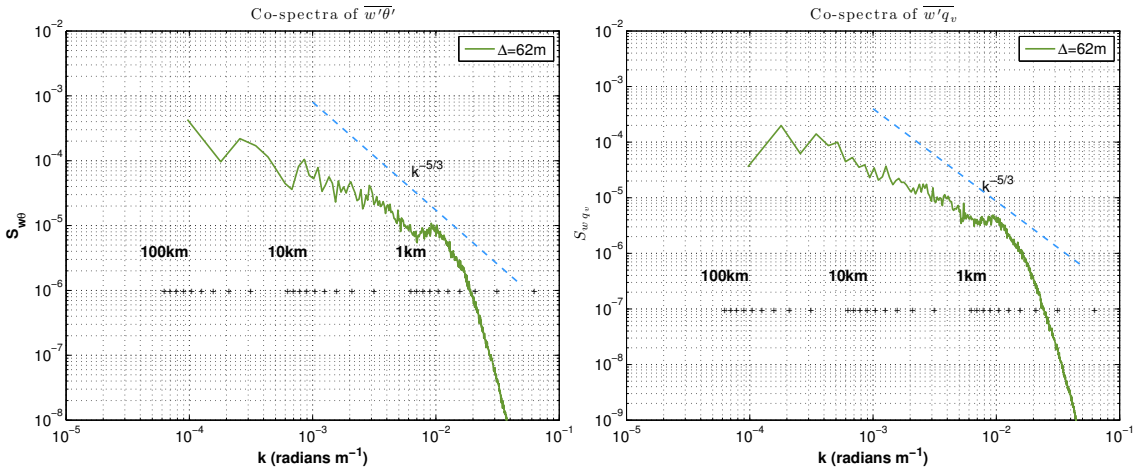

(a) $\overline{w'\theta'}$ **(b)** $\overline{w'q'_v}$

Figure 3.4.4: cospectra of $\overline{w'\theta'_v}$ (*unit:* Kms^{-1})and $\overline{w'q'_v}$ (*unit:* $gkg^{-1}ms^{-1}$) momentum flux respectively

4

Sub-Filter-Scale (SFS) Turbulence and Characteristics

In chapter 3, we saw that the SGS turbulence parameterization schemes in current operational forecasting models may not be able to represent the effect of SGS turbulence accurately. In this chapter we will investigate the influence of SGS turbulence parameterization schemes in the WRF-ARW model on the hurricane intensity forecasting by comparing SGS turbulence computed using parameterization schemes (*viz.* 2D-3D Smagorinsky scheme and 1.5 order TKE closure) with the explicitly computed sub-filter scale (SFS) turbulence.

4.1 Scale separation

To examine the effect of turbulence explicitly on the evolution of mean flow we spatially separated the velocity and the scalar meteorological fields into a resolved scale and sub-filter scale. Spatial filters provide ways to separate atmospheric fields based on the definition of certain wave number ranges. There are several methods to employ spatial filtering, for instance Fourier filtering, the discrete cosine transform(DCT), and digital filters. These different methods are characterized by different levels of performances and usability depending on the application. The discrete cosine-filter method has advantages in describing spatial trends but suffers from artificial wavy contributions (Denis et al., 2002). Digital filters operate within a finite base and can be constructed flexibly but have the disadvantage of being less effective in scale separation than Fourier filters (Feser and

von Storch, 2005; Shapiro, 1975). With respect to the frequency characteristics, the applied filter range determines the temporal and spatial features that will be identified. For a low-pass filter, the long waves will be retained, whereas a high-pass filter will remove contributions of long waves and short-wave systems will be conserved. Spatial filters are often applied in the context of storm or cyclone identification to remove the influence of atmospheric large-scale circulation, i.e. the planetary waves (Hoskins and Hodges, 2002; Anderson et al., 2003) or to select the spatial scales of interests, especially for tracking mesoscale and small-scale lows. To separate the flow spectrally, spatial filters are used to extract mesoscale features from the full fields. In the current study, we have used the discrete cosine transform (DCT) based on the discrete Fourier transform with a symmetrization process (Denis et al., 2002).

When the Fourier cut-off filter is applied over a limited area, it shows the problems associated with trend-contaminated time series, related to artificially adding wave contributions (Denis et al., 2002; Feser and von Storch, 2005). This results in the destruction of the normal spectrum and leads to distortion. DCT based on the discrete Fourier transform with a symmetrisation process (Denis et al., 2002) reduces this feature, but does not allow for full elimination. This process will be implemented by using the original function as a mirror image before applying the Fourier transform. Then this special Fourier transform is called the discrete cosine transform (DCT), employed as filter procedure in scale separation of mean flow within HBL.

An algorithm of spectral computation has been coded, based on an earlier (Denis et al., 2002) study, which used a discrete cosine transform (DCT) (Ahmed and Rao, 1974) to convert grid point fields into spectral fields. The advantage of DCT is that, unlike spectral computations based on Fast Fourier Transform (FFT), the meteorological fields do not need any trend removal to ensure periodicity (Erico, 1985). Moreover, (Denis et al., 2002) has shown that there is no aliasing on the large scale. Considering the typical resolution for an operational NWP model for hurricane forecast is about 1$\sim$2km, we choose a cut-off wavelength L_c'=1500m in DCT to decompose the flow in LES data into small-scale ($L_s \leq$1500m) and large-scale ($L_l \geq$1500m) flows. As indicated in Fig. 4.1.1, the flows with scales between the cut-off wavelength L_c'=1500m and the grid size L_c=62m are defined as Sub-Filter-Scale (SFS) turbulence. Chapter 3 has shown that the LES

has resolved the most energetic SFS motions. But they are SGS processes for a NWP model thus parameterization schemes are required to represent their effects on resolved scales. Assuming the SGS turbulent effect in the LES ($L \leq$62m) on the large-scale flow ($L \geq$1500m) is negligible comparing to the SFS motions, we can then evaluate the SGS parameterization schemes by comparing the parameterized turbulent stresses to those directly calculated using the SFS motions.

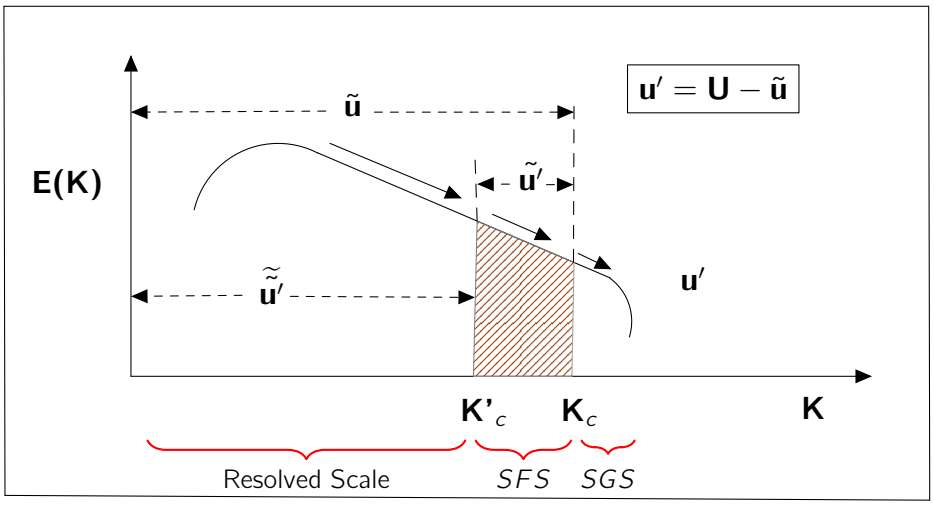

Figure 4.1.1: Scale separation of the flow with cut-off wavenumber $K'_c = 2\pi/L'_c$, where L'_c=cut-off wavelength(meters) and K_c=grid scale wavenumber (*unit:* m^{-1})

Figure 4.1.2, shows the structure of small-scale turbulent energetic eddies at model level-1 obtained after spectral decomposition of the flow using DCT filtering. The spectral filtering shows the intensity and structure of small-scale turbulent eddies are non-negligible, with maximum wind speed $\approx 40 ms^{-1}$. It is imperative to represent the influence of these turbulent eddies effectively into turbulence parametrization schemes in order to improve the hurricane intensity forecasting.

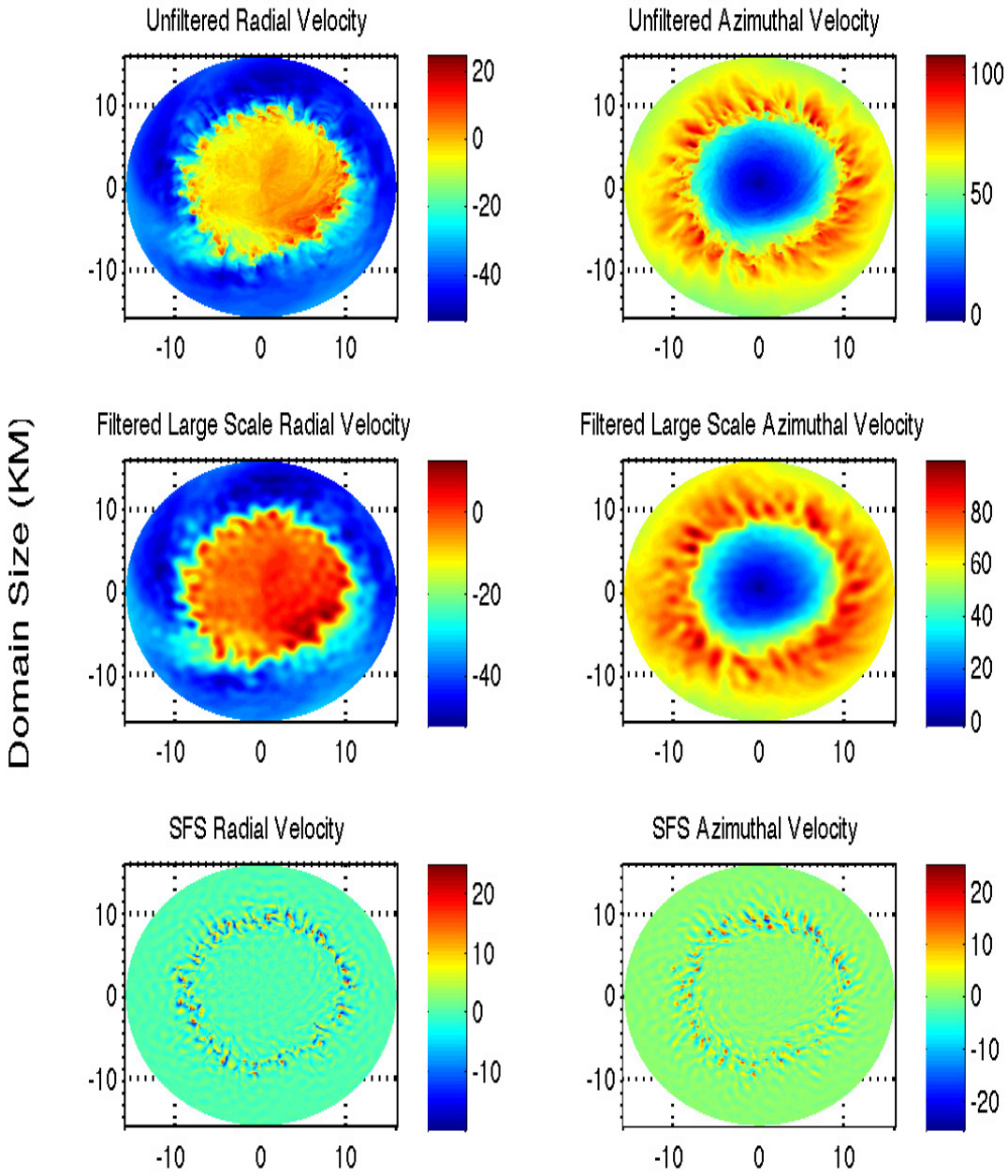

Figure 4.1.2: Spectral decomposition of mean flow into SFS $L_s < 1500$ and filtered large-scale $L_l > 1500m$, where X and Y-axis denotes the distance (*unit:* km) from the hurricane centre.

4.2 Turbulence characteristics of HBL

The PBL is the region of the atmosphere near the surface where the influence of the surface is felt through exchange of momentum, heat and moisture. The equations which describe the large-scale evolution of the atmosphere do not take into account the interaction with the surface. The turbulent motion responsible for this interaction is small-scale and totally sub-grid for current models and therefore needs to be parameterized. Hence, detail study of the turbulence structure is crucial to the parametrization of the hurricane boundary layer.

The WRF-LES experiment provided the data sets that contain resolved vertical and horizontal turbulence throughout the hurricane boundary layer. In this section, the vertical profiles of mean quantities and turbulent fluxes of velocity, heat and moisture are investigated by using the WRF-LES data in order to understand the dominant scales of variability related to the turbulent fluxes.

4.2.1 Vertical Structures of Turbulent Fluxes

The comparison of the vertical profiles of momentum, heat and moisture fluxes has been done by calculating the SFS turbulence fluxes. The fluxes of momentum, heat and humidity have been calculated using the eddy correlation method as follows:

$$\hat{\tau} = \rho(-\overline{w'u'}\,\hat{\mathbf{i}} - \overline{w'v'}\,\hat{\mathbf{j}}), \tag{4.1}$$

$$H = \rho c_p \overline{w'\theta'}, \tag{4.2}$$

$$E = \rho L_v \overline{w'q'} \tag{4.3}$$

where prime indicates SFS turbulent fluctuations; u', v', w', θ' and q' represent radial, azimuthal and vertical wind components, potential temperature, and specific humidity, respectively (until specified so); ρ represents the air density; c_p the specific heat at constant pressure; L_v the latent heat of vaporization; and an overbar represents the averages over the entire domain for every model level. The large SFS turbulent momentum fluxes near the surface are caused by the small-scale turbulence generated by the strong wind shear

in the surface layer. On the other hand, the resolved turbulence is responsible for most of the heat and moisture transport. The momentum fluxes in the azimuthal direction are the largest among the variances except for the upper part of the HBL Fig. 4.2.1(a) and (b). All the momentum fluxes have a maximum values near the surface and decrease with increasing height. The vertical flux of the azimuthal velocity $\overline{v'w'}$ has a minimum right above the surface and increases linearly to zero near the top of the HBL. This negative correlation infers that the azimuthal velocity tends to be stronger (weaker) in the downdraft (updraft) regions throughout the HBL. The vertical flux of the radial velocity $\overline{u'w'}$ is negative in most of the HBL, but shows positive values below few hundred meters from the surface in the HBL. The minimum of $\overline{u'w'}$ appears near the middle of the HBL. The distribution of the correlation $\overline{u'v'}$ is of a nearly reversed shape for that of $\overline{u'w'}$.

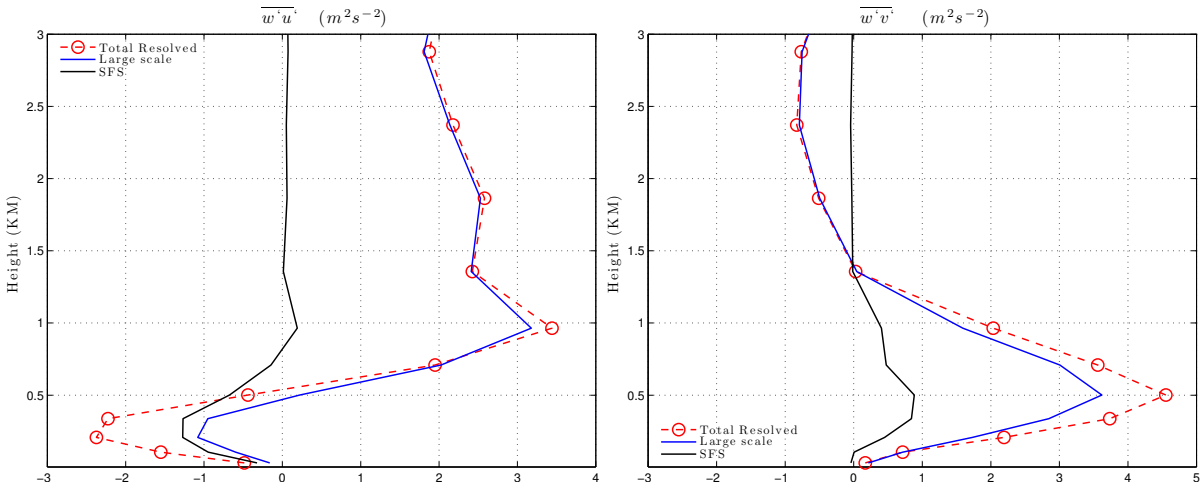

(a) vertical profile of $\overline{w'u'}$ **(b)** vertical profile of $\overline{w'v'}$

Figure 4.2.1: Vertical profiles of total SFS momentum fluxes.

4.3 TKE Budget

Evolution of the turbulence in the HBL assumes special importance because it plays a major role in the transportation of the heat and moistures from the surface to the higher levels of the atmosphere. Turbulent kinetic energy, which is a measure of turbulence in the atmosphere, is directly related to the transport of momentum, heat, and moisture through the boundary layer. Thus, understanding the variation of the individual budget components is crucial for energy exchange mechanism within HBL. The TKE budget equation is commonly used to parameterize turbulent properties of the surface layer in large scale atmospheric models (Frenzen and Vogel, 1992). The TKE budget associates the local storage of turbulence to the shear production, buoyancy production, dissipation, and the transport processes and has numerous applications in both empirical and computational modeling in boundary-layer meteorology (Holza and Robins, 2004).

A study of the TKE budget under unstable conditions and convective conditions is important for understanding the structure of HBL. It was found in (Caughey and Wyngaard, 1979) that in the unstable surface layer, all terms in the TKE budget are considerable, and TKE generated through buoyancy forces is transported out of the boundary Layer (BL), while the dissipation rate can be regarded as an approximation of the sum of mechanical production and the residual terms of TKE budget. Results at different sites about TKE budget and dissipation are emphasizing the importance of various TKE terms during convective situations and the necessity to be included in numerical weather prediction models, particularly in models that resolve mesoscale structures (Tyagi and Satyanarayana, 2013).

The high-resolution data generated by WRF-LES allow us to diagnose the budget of variance and covariance of the resolved turbulence. To study the nature of turbulence production and destruction within HBL; we have estimated the TKE budget by using following formula (Zhu, 2008).

$$\frac{\partial \overline{e}}{\partial t} = -\overline{\widetilde{U}_j}\frac{\partial \overline{e}}{\partial x_j} - \overline{u_i' u_j'}\frac{\partial \overline{\widetilde{U}_i}}{\partial x_j} + \frac{g}{\overline{\theta}}\left(\overline{w'\theta_v'}\right) - \frac{\partial \overline{u_j' e}}{\partial x_j} - \frac{1}{\overline{\rho}}\frac{\partial \overline{u_j' p'}}{\partial x_i} - \epsilon, \tag{4.4}$$

u_i' and $\widetilde{U}_i (i = x, y, z)$ is the SFS and filtered large-scale velocity components resp. along three directions in Cartesian coordinates and p' is the SFS pressure. The overbar repre-

sents the domain and time mean of a generic variable, where $\overline{e}$ is the turbulent kinetic energy and defined as $\overline{e} = \frac{1}{2}\overline{u_i'^2}$, and ϵ is the dissipation rate of turbulent kinetic energy. Equation (4.4) has been written following Einstein summation convention.

The left hand side of Eq. (4.4) is the local rate of change of TKE or Storage term, terms on the right-hand side of the equation represent the TKE advection, shear production, buoyancy production, turbulent transport, pressure correlation or mechanical production, and dissipation rate. An examination of the terms in the turbulent kinetic energy equation could help our understanding of the nature of turbulent production and destruction in the boundary layer. The terms which has not been calculated from the LES data (i.e. the dissipation rate (ϵ)) have been lumped together to form a residual term (R_{TKE}) which takes on the value required to satisfy the Eq. (4.4).

The TKE is one of the most important variables because it measures the intensity of turbulence. It is directly related to the momentum, heat and moisture transport from the surface through the boundary layer. Combining all the terms computed using Eq. (4.4), Fig. 4.3.1 shows the TKE budgets of the hurricane boundary layer averaged over 90 seconds for the domain size of 15kmx15km.

Figure 4.3.1 shows that the TKE budget is primarily dominated by the shear production because of the strong hurricane shear environment but decreases rapidly with increasing altitude in the lower half of the boundary layer. The magnitude of the shear production term decreases with height because of the weak gradient of velocity stress tensors and the decrease in wind shear with height.

The most remarkable feature shown in the TKE budget is the large advection term, which nearly balances the shear production term. The large advection is caused by the combination of the strong hurricane winds and an inhomogeneity of SFS turbulent winds. The magnitude of advection of SFS turbulent kinetic energy by the mean winds is negative upto $\sim 300m$ height and became positive afterwards with increasing altitude. The horizontal momentum fluxes are stronger than the vertical momentum fluxes within the lower 300m of the HBL and transport turbulent kinetic energy in a horizontal direction. These fluxes act like a sink of TKE. Above 300m altitude, the vertical fluxes seem to be the more dominant turbulent fluxes and transport turbulent kinetic energy in upward

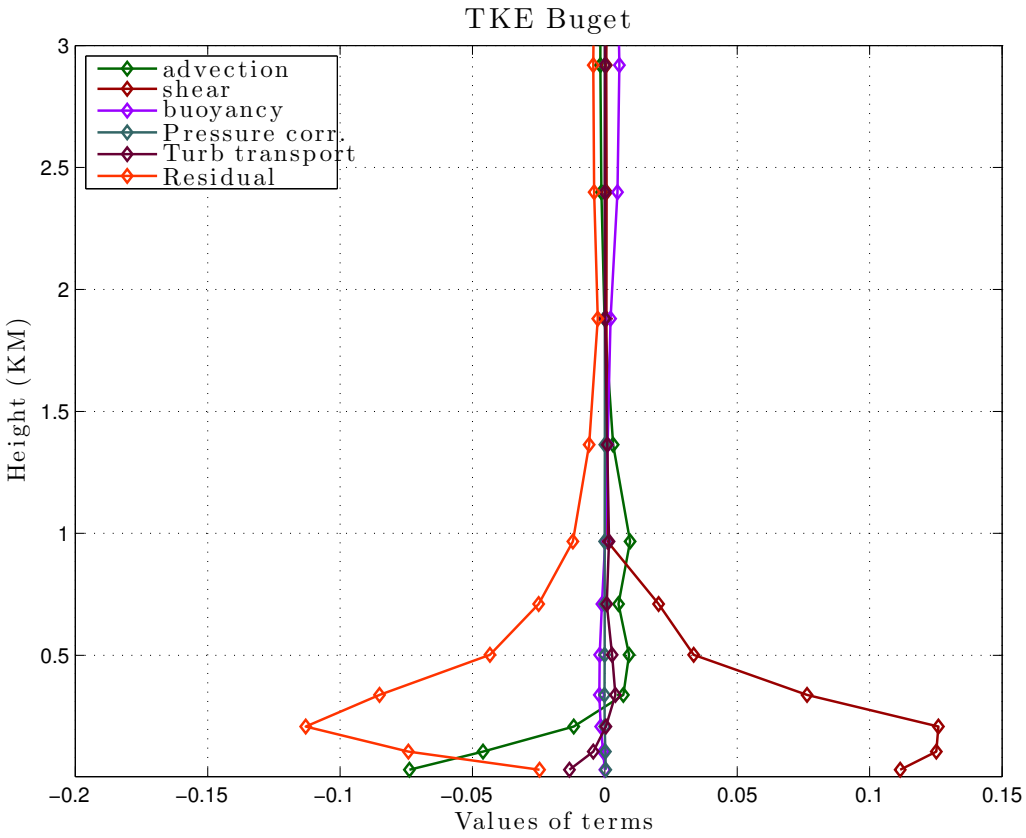

Figure 4.3.1: Vertical profiles of TKE budget terms

direction by the resolved velocity and acts like a source of TKE. Direct measurements and observations are not available for measuring advection terms within HBL but we can speculate that the advection term is important source of turbulent kinetic energy within HBL.

At the lowest level, the buoyancy term is generally an order of magnitude smaller than the shear production and advection terms, and while the latter decreases rapidly with height the buoyancy production term changes little with height and indicates a near-neutrality of the boundary layer. The most important part of the buoyancy term is the flux of virtual potential temperature $\overline{w'\theta'_v}$, which measures the flux of heat. At intermediate and higher levels the buoyancy production is the dominant term because of the larger moisture flux.

The pressure correlation term decreases with increasing altitude and is one order of magnitude smaller than the rest of the TKE budget terms. In general the pressure correlation term not only acts to redistribute TKE within boundary later, but it can also drain energy out of boundary layer (Stull, 1988).

The transport terms are usually assumed to be small, but it has been seen here that the sum of the pressure correlation term and the nonlinear local turbulent transport term is an important source for the turbulent kinetic energy. On a local scale the turbulent transport term acts like either a production or loss, depending upon whether there is a flux convergence or divergence, so overall this term does not create or destroy TKE, it just moves or distributes TKE from one location to another (Stull, 1988). The turbulent transport term represents the flux divergence of TKE for a layer since it depends on the vertical gradient of the TKE flux. So, for a given layer, if more flux is entering the layer than leaving it, and there is a net convergence of the vertical flux, then the TKE of the layer will necessarily increase. The magnitude of the turbulent transport term is non-negligible within the lower 500m of the HBL and compares to other terms of TKE budget.

4.4 Computation of Explicit SFS stresses

To investigate influence of turbulent eddies smaller than the grid size of current operational models with a cut off wavelength (L_c'=1500m) similar to the grid size of operational models has been chosen to separate flows using DCT, as described in section 4.1. Low-pass filtering the incompressible Navier-Stoke's equations result in:

$$\frac{\partial \tilde{u}}{\partial x_i} = 0, \tag{4.5}$$

$$\frac{\partial \tilde{u}_i}{\partial t} + \frac{\partial \widetilde{u_i u_j}}{\partial x_j} = -\frac{\partial}{\partial x_i}\left(\frac{\tilde{p}}{\rho}\right) + \nu \frac{\partial^2 \tilde{u}_i}{\partial x_j^2} \tag{4.6}$$

where $\tilde{\varphi}$ denotes a time, spatial or ensemble averaged or filtered variable. The filtered second-order momentum involves problems related to closure because this term consists of an unknown filtered product of velocities ($\widetilde{u_i u_j}$). Rewriting this term results in:

$$\widetilde{u_i u_j} = \tilde{u}_i \tilde{u}_j + \tau_{ij}, \qquad \tau_{ij} = \left(\widetilde{u_i u_j} - \tilde{u}_i \tilde{u}_j\right), \tag{4.7}$$

where τ_{ij} is the sub-filter kinematic Reynolds stress tensor:

$$\tau_{ij} = \begin{pmatrix} \tau_{11} & \tau_{12} & \tau_{13} \\ \tau_{21} & \tau_{22} & \tau_{23} \\ \tau_{31} & \tau_{32} & \tau_{33} \end{pmatrix} \tag{4.8}$$

The stress tensor is split into an isotropic part(normal stresses τ_{ii}, changing the volume) and a deviatoric part (τ_{ij} with $i \neq j$, deforming the volume) where the isotropic part is absorbed in a modified pressure π_i:

$$\tau_{ij} = \left(\widetilde{u_i u_j} - \tilde{u}_i \tilde{u}_j\right) - \frac{2}{3}\delta_{ij} e, \tag{4.9}$$

$$\pi_i = \frac{\tilde{p}}{\rho} + \frac{2}{3} e, \tag{4.10}$$

where δ_{ij} is the Kronecker delta and *'e'* the sub-filter kinetic energy:

$$e = \frac{1}{2}\tau_{ii} = \frac{1}{2}\left(\widetilde{u_i u_j} - \tilde{u}_i \tilde{u}_j\right), \tag{4.11}$$

Substitution of equations (4.9) - (4.11) into Eq. (4.6) results in:

$$\frac{\partial \tilde{u}_i}{\partial t} + \frac{\partial \tilde{u}_i \tilde{u}_j}{\partial x_j} = -\frac{\partial \pi}{\partial x_i} + \nu \frac{\partial^2 \tilde{u}_i}{\partial x_j^2} - \frac{\partial \tau_{ij}}{\partial x_j}, \tag{4.12}$$

Which still leaves τ_{ij} as an unknown variable and must be parametrized. To estimate the total stress due to interaction among the whole spectral range of turbulence; Leonard (1974) decomposed these stress tensors as

$$\tau_{ij} = L_{ij} + C_{ij} + R_{ij} = \widetilde{u_i u_j} - \tilde{u}_i \tilde{u}_j \tag{4.13}$$

Where,

$$L_{ij} = \widetilde{\tilde{u}_i \tilde{u}_j} - \tilde{u}_i \tilde{u}_j,$$
$$C_{ij} = \widetilde{\tilde{u}_i u_j'} - \widetilde{\tilde{u}_j u_i'},$$
$$R_{ij} = \widetilde{u_i' u_j'}$$

the physical interpretation for each term is given as follows; the Leonard stress tensor L_{ij}, represents interaction among large scales, the Reynolds stress-like term R_{ij}, represents interactions among the SFS, and the Cross-Stress Tensor C_{ij}, represents cross-scale interactions between large and SFS turbulence. In the current study, we have used sharp cut-off filter in the wavenumber space to separate the hurricane winds into small-scale and large-scale. The stress tensor terms C_{ij} and L_{ij} are identically zero, because of the implementation of sharp cut-off filter (Winckelmans et al., 1996). Therefore, the stress tensor can be explicitly computed using the SFS motions.

4.5 Estimation of SFS stress tensor using turbulence parameterization schemes

The spatial discretization of the WRF physical-space diffusion operators for the horizontal and vertical momentum equations are

$$\begin{aligned}
\frac{\partial U}{\partial t} &= \ldots \; - \left[\frac{\partial \tau_{11}}{\partial x} + \frac{\partial \tau_{12}}{\partial y} - \frac{\partial (Z_x \tau_{11} + Z_y \tau_{12})}{\partial z}\right] - \frac{\partial \tau_{13}}{\partial z} \\
\frac{\partial V}{\partial t} &= \ldots \; - \left[\frac{\partial \tau_{12}}{\partial x} + \frac{\partial \tau_{22}}{\partial y} - \frac{\partial (Z_x \tau_{12} + Z_y \tau_{22})}{\partial z}\right] - \frac{\partial \tau_{23}}{\partial z} \\
\frac{\partial W}{\partial t} &= \ldots \; - \left[\frac{\partial \tau_{13}}{\partial x} + \frac{\partial \tau_{23}}{\partial y} - \frac{\partial (Z_x \tau_{13} + Z_y \tau_{23})}{\partial z}\right] - \frac{\partial \tau_{33}}{\partial z}
\end{aligned} \tag{4.14}$$

$Z_x = g^{-1}\delta_x \phi$ and $Z_y = g^{-1}\delta_y \phi$ are the metric terms defined on w levels, and (Z_x, Z_y) are horizontally coincident with U and V. The components of stress tensors can be written as follows:

$$\begin{aligned}
\tau_{11} &= -\mu_d K_h D_{11} \qquad \tau_{12} = -\mu_d K_h D_{12} \qquad \tau_{13} = -\mu_d K_v D_{13} \\
\tau_{22} &= -\mu_d K_h D_{22} \qquad \tau_{23} = -\mu_d K_v D_{23} \qquad \tau_{33} = -\mu_d K_v D_{33}
\end{aligned} \tag{4.15}$$

Where K_h, K_v are horizontal and vertical eddy viscosities respectively. Symmetry sets the remaining tensor values; $\tau_{21} = \tau_{12}$, and $\tau_{31} = \tau_{13}$, and $\tau_{32} = \tau_{23}$. The stress tensor τ is calculated from the deformation tensor D. The continuous deformation tensor is defined as;

$$\begin{aligned}
D_{11} &= 2\left[\frac{\partial u}{\partial x} - Z_x \frac{\partial u}{\partial z}\right] \\
D_{22} &= 2\left[\frac{\partial v}{\partial y} - Z_y \frac{\partial v}{\partial z}\right] \\
D_{33} &= 2\frac{\partial w}{\partial z} \\
D_{12} &= \left[\frac{\partial u}{\partial y} - Z_y \frac{\partial u}{\partial z} + \frac{\partial v}{\partial x} - Z_x \frac{\partial v}{\partial z}\right] \\
D_{13} &= \left[\frac{\partial w}{\partial x} - Z_x \frac{\partial w}{\partial z} + \frac{\partial u}{\partial z}\right] \\
D_{23} &= \left[\frac{\partial w}{\partial y} - Z_y \frac{\partial w}{\partial z} + \frac{\partial v}{\partial z}\right]
\end{aligned}$$

The deformation tensor is symmetric, hence $D_{21} = D_{12}$, $D_{31} = D_{13}$, and $D_{32} = D_{23}$. In WRF-ARW, the eddy viscosity K_h and K_v can be determined in three closure schemes, namely 2D Smagorinsky closure, 3D Smagorinsky closure, and prognostic TKE closure. Horizontal eddy viscosity K_h can be determined from the horizontal deformation using a Smagorinsky first-order closure. In these formulation, the eddy viscosity is defined as

$$K_h = C_s^2 l^2 \left[0.25 \left(D_{11} - D_{22}\right)^2 + D_{12}^2\right]^{\frac{1}{2}} \tag{4.16}$$

The deformation tensor components have been defined in the previous section. The length scale is $l = (\Delta x \Delta y)^{1/2}$ and C_s is a dimensionless number called as *Smagorinsky Constant*. This option is most often used with a planetary boundary layer scheme that independently handles the vertical mixing. The real case simulation in Ch. 2 has used this option.

4.5.1 3D Smagorinsky Closure

The horizontal and vertical eddy viscosity (K_v) can be determined using a 3D Smagorinsky turbulence closure. This closure specifies the eddy viscosities as

$$K_{h,v} = C_s^2 l_{h,v}^2 max \left[0., \left(D^2 - P_r^{-1} N^2\right)^{1/2}\right], \tag{4.17}$$

where

$$D^2 = \frac{1}{2}\left[D_{11}^2 + D_{22}^2 + D_{33}^2\right] + D_{12}^2 + D_{13}^2 + D_{23}^2, \tag{4.18}$$

and **N** is the Brunt-Väisälä frequency. An isotropic length scale when ($\Delta x, \Delta y \simeq \Delta z$) can be estimated by $l_h = (\Delta x \Delta y \Delta z)^{1/3}$; whereas for an anisotropic turbulence ($\Delta x, \Delta y >> \Delta z$), the horizontal length scale $l_h = (\Delta x \Delta y)^{1/2}$ and vertical length scale $l_v = \Delta z$ for estimation of K_h and K_v respectively.

4.5.2 Prognostic TKE Closure

For the predicted turbulent kinetic energy (TKE), the eddy viscosities are computed using

$$K_{h,v} = C_k l_{h,v} \sqrt{e}, \tag{4.19}$$

where e is the TKE (a prognostic variable in the scheme), C_k is a constant (typically $0.15 < C_k < 0.25$, and $l_{h,v}$ is the length scale. An isotropic turbulence length scale be determined from,

$$\begin{aligned} l_{h,v} = min\left[(\Delta x \Delta y \Delta z)^{1/3}, 0.76\sqrt{e}/N\right] \qquad & for N^2 > 0, \\ l_{h,v} = (\Delta x \Delta y \Delta z)^{1/3} \qquad & for N^2 \leq 0 \end{aligned} \tag{4.20}$$

An anisotropic turbulence length scale can be determined follows;

$$\begin{aligned} l_v = min\left[\Delta z, 0.76\sqrt{e}/N\right] \qquad & for N^2 > 0, \\ l_v = \Delta z \qquad & for N^2 \leq 0. \end{aligned} \tag{4.21}$$

By substituting SFS stress tensor computed using Eq. (4.13) and (4.15) into the last term of equation (4.12) or (4.14) we can investigate the momentum transfer due to stresses. Also, we can compare the parameterized and explicitly computed stresses to examine the contribution of each in the evolution of large-scale flow/eddies.

4.6 Comparison of parameterized and explicit SFS turbulences

As discussed in section 4.4, by using Eq. (4.12) and (4.14), the gradient of SFS turbulence stress tensor ($\frac{\partial \tau_{ij}}{\partial x_j}$) (where τ_{ij} is the SFS turbulence stress tensor, x_j the direction (x,y,z) in Cartesian coordinates) have been computed explicitly using the WRF-ARW model turbulence parameterization schemes. For the numerical simulations where the model grid-size (Δ) is same as the filter scale (L_c'), the total stress becomes the sub-grid scale turbulence stress, which will then need to be parameterized. For convenience in hurricane dynamics, the gradient of SFS turbulence stress tensor can be transformed from Cartesian coordinates to cylindrical coordinates with the radial (r), azimuthal (θ) and vertical (z) directions.

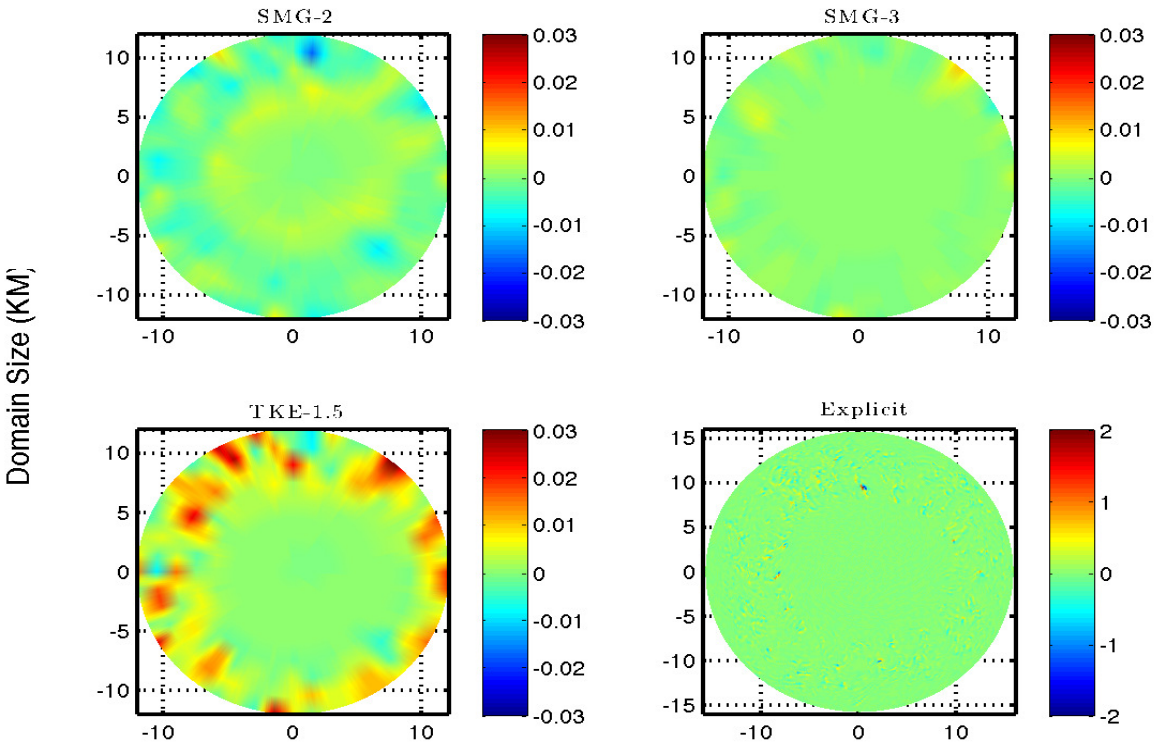

Figure 4.6.1: Gradient of SFS stress tensors (*unit:* ms^{-2}) along azimuthal direction estimated at $\sim 120m$ above the surface, the X and Y-axis represents the distance (*unit:* km) from the hurricane center.

Figures 4.6.1 and 4.6.2, shows the gradients of SFS turbulence stress tensor ($\frac{\partial \tau_{ij}}{\partial x_j}$) along tangential and radial direction respectively at height $\sim 120m$ from the surface. The magnitude of the explicitly computed ($\frac{\partial \tau_{ij}}{\partial x_j}$) is two order larger than that of turbulence

parameterization schemes (Smagorinsky-2D (τ_{smg2})[1], Smagorinsky-3D (τ_{smg3}) and TKE-1.5 order closure (τ_{tke})). Note that Smagorinsky-2D scheme only contains horizontal turbulence mixing, while the other two include vertical mixing.

The structure of estimated ($\frac{\partial \tau_{ij}}{\partial x_j}$) using parameterization schemes is very smooth and coarse. In contrast, the structure of explicitly estimated ($\frac{\partial \tau_{ij}}{\partial x_j}$) shows much finer scale and energetic eddies within the HBL. The difference in structure is expected because the parameterization schemes use the filtered motions sampled on a grid with resolution similar to filtered scale i.e. $\Delta x = L'_c$=1500m and SFS motions on a grid with Δx=62m respectively (c.f. Fig. 4.1.2). Even though the winds in the filtered scale are larger, their gradients are not as strong as that of the SFS winds.

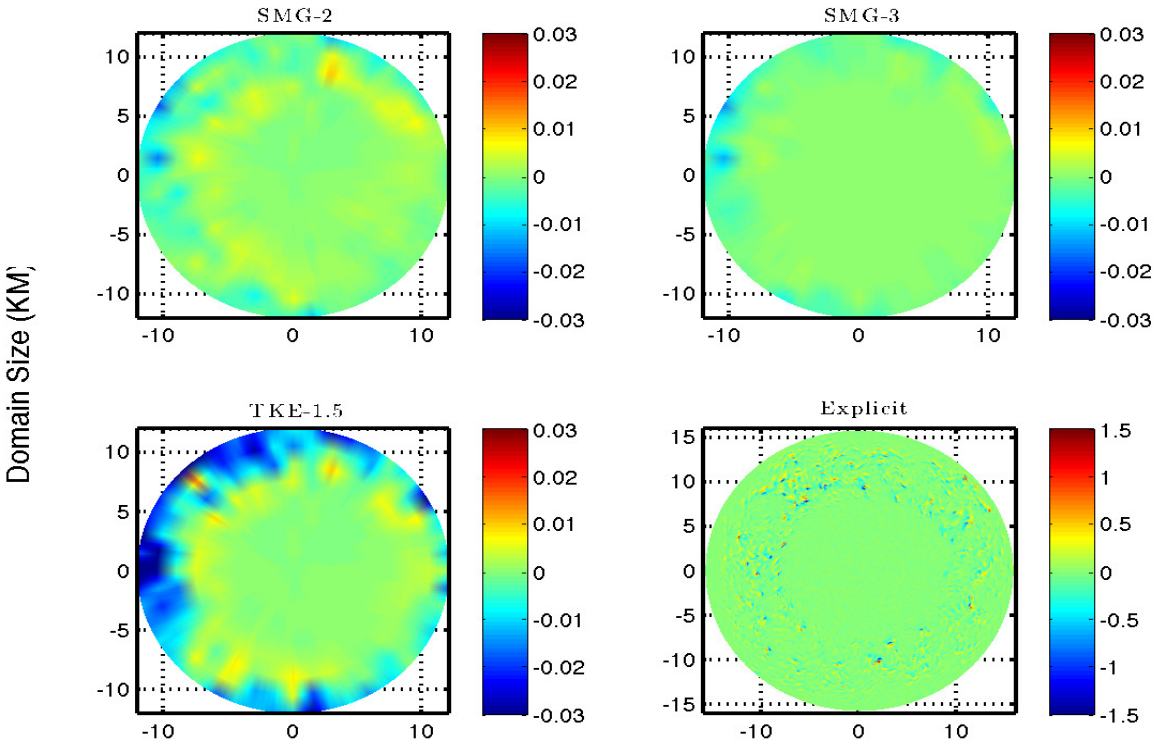

Figure 4.6.2: Same as Fig. 4.6.1 but along radial direction.

Figures 4.6.3 and 4.6.4, shows the vertical structure of the azimuthal mean ($\frac{\partial \tau_{ij}}{\partial x_j}$) in the azimuthal and radial directions respectively. Taking the azimuthal mean indicates

[1]In WRF-ARW model, the τ_{smg2} turbulence parametrization scheme estimates the turbulence mixing along horizontal direction only, while vertical mixing has been taken care by the Planetary Boundary Layer (PBL) schemes. In the current study, for τ_{smg2} turbulence parametrization scheme, the gradient of turbulent stress tensor along horizontal direction has been computed only

the effect of turbulence on the mean azimuthal and radial winds. The azimuthal mean $(\frac{\partial \tau_{ij}}{\partial x_j})$ computed explicitly and by using parameterization schemes have approximately the same order of magnitude, but the explicitly computed $(\frac{\partial \tau_{ij}}{\partial x_j})$ shows very strong and coherent turbulent eddies within HBL. The azimuthal mean $(\frac{\partial \tau_{ij}}{\partial x_j})$ in the azimuthal direction is negative upto =100-200m from the surface. Note that the horizontal or vertical derivatives of the stresses give the momentum sinks/sources. The SFS turbulence tend to slow down the near surface mean azimuthal wind but accelerate the wind immediately above the surface layer. The magnitude of the azimuthal mean $(\frac{\partial \tau_{ij}}{\partial x_j})$ in the azimuthal direction estimated using Smagorinsky-2D and Smagorinsky-3D parameterization schemes are relatively weaker in magnitude compared to the explicit and TKE-1.5 order closure azimuthal mean. The main acceleration/deceleration occurs in HBL.

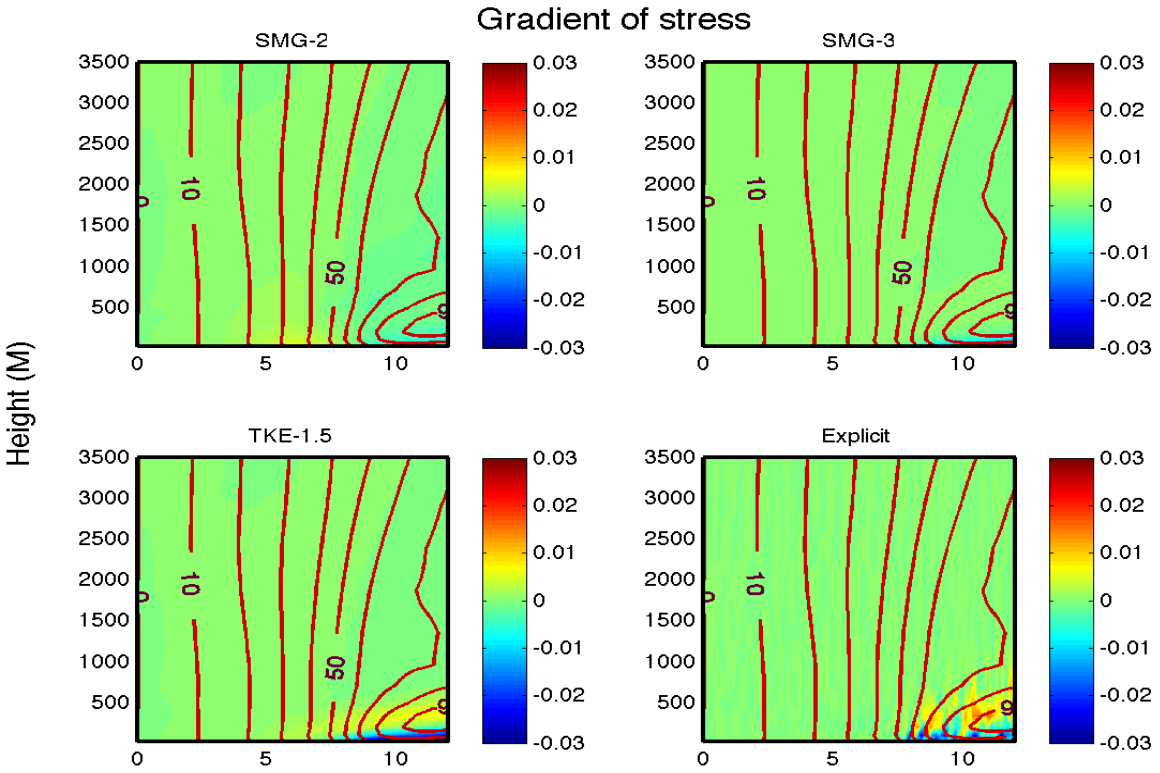

Figure 4.6.3: Vertical structure of the azimuthal mean gradients of SFS and parameterized stress tensors along azimuthal direction (color shading) and the mean azimuthal wind (contour intervals 10 ms^{-2}). X-axis represents the hurricane radius (*unit:* km).

Figure 4.6.4 shows that the explicit SFS turbulence mixing tends to slow down the radial inflow near surface and the returning radial outflow. The SGS parameterization schemes produce similar patterns in the surface layer within HBL, but their magnitudes

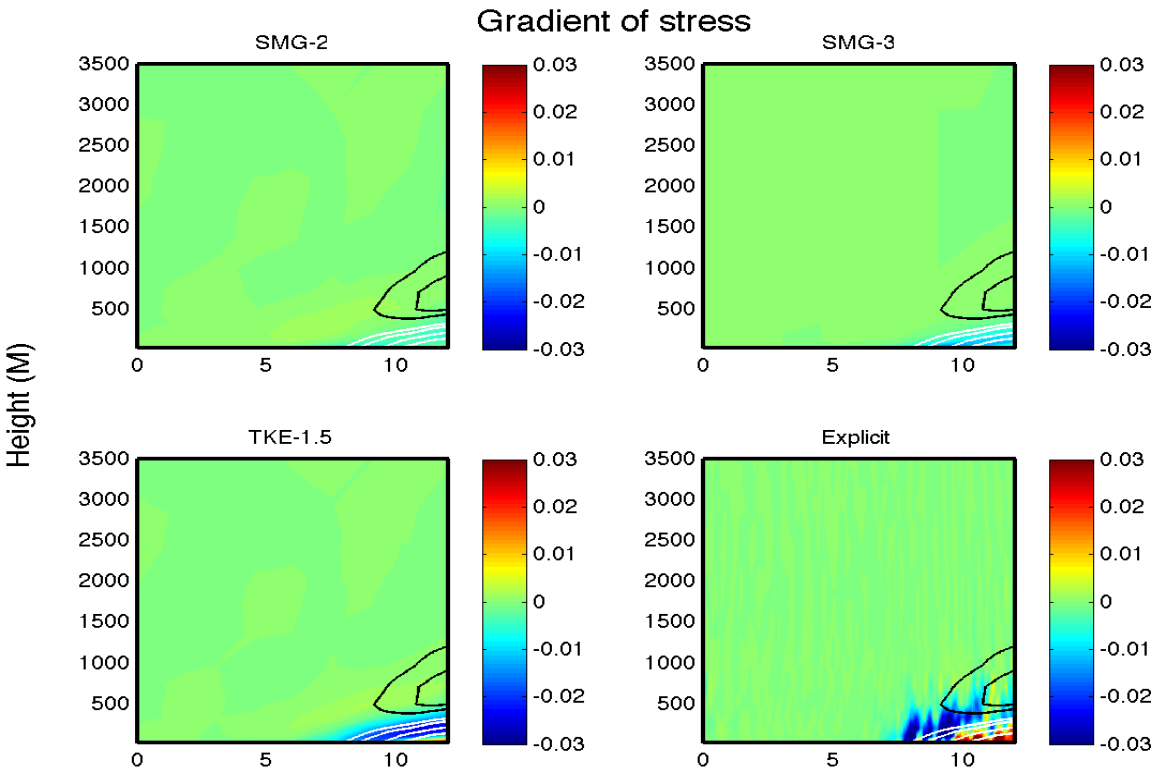

Figure 4.6.4: Same as Fig. 4.6.3 but along radial direction, Contours are azimuthal mean radial wind plotted at -30, -20, -10, -5, 5, and 10 ms^{-2}, positive values in black, and negative values in white.

are not nearly as strong, especially the deceleration of the inflow (positive tendency).

The vertical profile of mean gradient stress tensor along azimuthal and radial directions are shown in Fig. 4.6.5. The vertical profile of the averaged gradient of the explicit SFS stress tensor along the azimuthal direction is negative upto $\sim 250m$ height within HBL and becomes positive afterwards till $\sim 1000m$ height. In the radial direction, the explicit SFS turbulence diffusion decelerates the radial inflow below $\sim 150m$ and accelerates the radial outflow above it until about 1000m. These results are consistent with a recent study by Rotunno and Bryan (2012) who revisited the rotating flow boundary layer problem. It was solved analytically by Bödewadt in 1940 Schlichting (1996) and Kuo (1971) showed the turbulence tends to counteract the mean circulation.

In contrast, the TKE-1.5 order closure scheme produces too much turbulence dissipation on the azimuthal wind while the dissipation produces by of 2D-Smagorinsky scheme is negligible. The 3D smagorinsky scheme matches the magnitude of the explicit value, but it fails to generate positive tendency above the surface layer. The TKE-1.5 order SGS

parameterization scheme and explicit SFS turbulence on average decelerate strong near surface inflow but the TKE scheme is too dissipative just above the surface layer. Reducing diffusivities in the TKE scheme maybe one simple remedy to improve the representation of the turbulence effects on the mean flow.

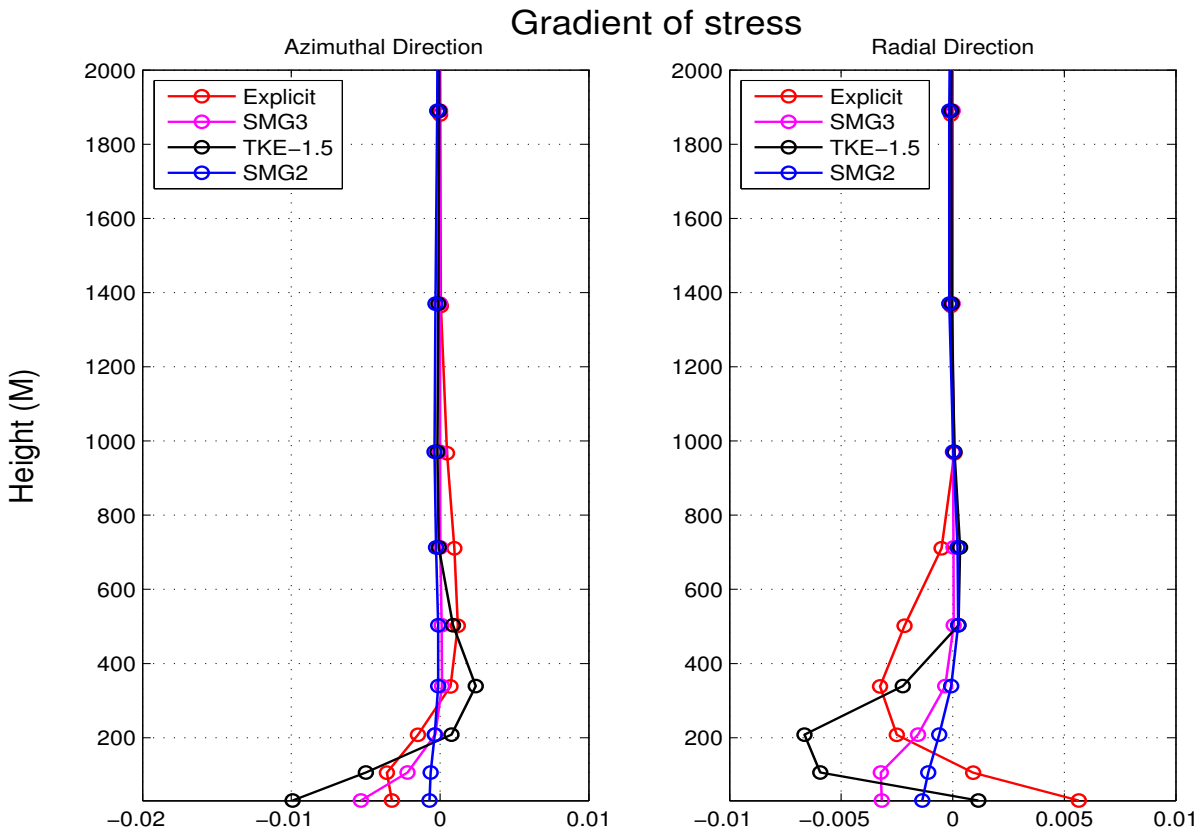

Figure 4.6.5: Vertical profile of mean gradient of stress tensor (*unit:* ms^{-2}) along azimuthal and radial direction over the entire domain of size 15x15km

4.7 Computation of mixing length scale ($l_{h,v}$)

The most popular and widely used turbulence parameterization schemes (*viz.* Smagorinsky model in the context with WRF-ARW model) have a few shortcomings (dependent on the empirical constant C_s, also these schemes can not capture the energy backscatter or upscale energy cascading effect) and perform well for isotropic and statistically homogeneous turbulence. The HBL structure is very different from normal atmospheric boundary layer, because HBL is associated with strong winds and intense turbulent exchange of heat, moisture and momentum between Air-Sea interface. This could be the possible reason for poor performance of Smagorinsky turbulence parametrization schemes within HBL. As indicated in the previous section, a simple remedy to improve turbulence representation in the Smagorinsky scheme is to change its diffusivity. It can be done by changing the Smagorinsky constant C_s or the mixing length scale $l_{h,v}$. In this section, the proper turbulence mixing length scale will be estimated using the SFS motions.

The mixing length scale ($l_{h,v}$) is a virtual scale in numerical models and is quantitatively smaller than the energy-containing scale of turbulent eddies. The distinction between these two scales is a useful reminder for the modeling community on the representation of small-scale turbulence in hurricanes. The mixing length (l_h) relates the eddy-viscosity(K_h) coefficient with the turbulent velocity as described in section 4.5. In the WRF-ARW model the horizontal mixing length scale l_h is typically represented by the grid size i.e. $l_h = (\Delta x \Delta y)^{1/2}$, $l_v = (\Delta x \Delta y \Delta z)^{1/3}$. Representation of mixing length in terms of grid size is not a good approximation as discussed in Chapter 2, because C_s acts as a ratio of a mixing length scale l_h to a grid scale,$C_s = l_h/\Delta$. It has been observed in Chapter 2 that simulations with a fixed grid length showed a strong dependence on C_s, because large values C_s produced weak hurricanes and vice versa.

The simplest model proposed by Smagorinsky (1963) has been used to compute the horizontal mixing length scale, utilizing filtered velocity and explicitly computed stresses. The linear eddy-viscosity model proposed by Smagorinsky (1963), is given as

$$\tau_{ij} = -2\nu_r \overline{\mathbb{S}} \tag{4.22}$$

where $\overline{\mathbb{S}}$ is the characteristic filtered rate of strain determined from $\overline{\mathbb{S}} = (2\overline{S}_{ij}\overline{S}_{ij})^{1/2}$, where $\overline{S}_{ij}$ is filtered rate-of-strain tensor given by

$$\overline{S}_{ij} = \frac{1}{2}\left(\frac{\partial \widetilde{U}_i}{\partial x_j} + \frac{\partial \widetilde{U}_j}{\partial x_i}\right) \tag{4.23}$$

where $\widetilde{U_{ij}}$ is large-scale filtered velocity and ν_r is the eddy-viscosity of the SFS motions. By analogy with the mixing-length hypothesis, the eddy-viscosity is modelled as

$$\nu_r = l_h^2\overline{\mathbb{S}} = (C_s\Delta)^2\,\overline{\mathbb{S}}, \tag{4.24}$$

where C_s is Smagorinsky constant.

In order to compute l_h, we explicitly computed SFS turbulence stress tensor τ_{ij}, and substitute it into equation (4.22) to compute eddy viscosity. The mixing length has been estimated by substituting eddy-viscosity into equation (4.24) for $C_s = 0.25$ (we are assuming here $C_s = 0.25$, which is a default value for Smagorinsky Constant in WRF-ARW model).

The estimated average value of horizontal mixing length scale is L_h ~3000m within 1km of the HBL. Note that our definition of L_h is different from the estimated value of mixing length l_h by (Zhang and Montgomery (2012), eq. 5), because in WRF model l_h has estimated by a factor of C_s i.e., $l_h = C_s L_h = 0.25x3000 \sim 750m$. The estimated value of l_h using WRF-LES is consistent with the estimated value of l_h ~700m, l_h ~1.5km by Zhang and Montgomery (2012) from aircraft observations and Rotunno and Bryan (2012) from axisymmetric model respectively.

From both theoretical and practical perspectives, the observational evidence suggests that a constant horizontal mixing length may be adequate in simple theoretical models and in numerical hurricane models. The horizontal mixing length is approximately 7 times the vertical mixing length (Zhang and Montgomery, 2012). The estimated horizontal eddy diffusivity (*as discussed in section 4.5*) is found to increase somewhat with wind speed. The $l_h \sim 750m$ is the average mixing length estimated over the hurricane eyewall region where winds are very strong, so that, this value would appeared to be the reasonable estimates of l_h to used for the hurricane forecasting with gridlength $\sim 3km$ if the $C_s = 0.25$. In the

real case simulation in Ch. 2, a reasonable C_s should be 0.56 since the grid resolution is 1.33 km. However the simulation with the closest C_s value (0.5) did not produce the best intensity forecast. It suggests that physical processes other than HBL turbulence are also important in determining the hurricane intensity.

5

Summary and Future Scope

We have used the WRF-ARW model to investigate the sensitivity of turbulence on hurricane intensity and track by simulating a real case Hurricane Danielle(2010). It has been observed that the intensity for Hurricane Danielle(2010) are sensitive to both the model resolution (Δx) and horizontal mixing length scale (l_h). If the model resolution is higher, WRF-ARW produces strong hurricane and vice versa. Similarly, it has been also observed that, as the magnitude of l_h decreases by keeping minimum C_s, the intensity of the simulated hurricane increases and vice versa. The significant changes has not been observed in the simulated tracks of Hurricane Danielle(2010) with respect to the variations of Δx and C_s. The vertical structures of simulated Hurricane Danielle(2010) change dramatically with the varying C_s. When C_s is small, the vertical structure of the azimuthal component of wind velocity is relatively compact and strong because the near surface radial winds produce stronger convergence and in turn the hurricane becomes more intense. For large values of C_s the depth of radial inflow of winds is taller but the convergence in the eyewall is weaker compared to lower values C_s. The formation of secondary eyewall has been also observed for the smaller values of C_s in the simulation of Hurricane Danielle(2010). In summary, the WRF-ARW model simulated Hurricane Danielle(2010) intensity forecasting shows sensitivity to the horizontal turbulence mixing.

It is until the grid resolution increases to $\Delta x = 62m$ the the kinetic energy spectra has clearly produced the inertial subrange region where the turbulence has considered to be statistically steady, homogeneous and cascade down the large scale TKE to the small scales. The largest scale of the energetic eddy which cascades the TKE to the smaller-scales has found to be of the size $\approx 3.5km$. The kinetic energy spectra for the coarser

domain with resolution $\Delta x = 1.67m$ down to $\Delta x = 550m$ had failed to capture the inertial subrange region possibly because of an inefficiency of the turbulence parameterization schemes to capture the turbulent eddies. The WRF-LES produced the energy spectra and cospectra for the heat, momentum and moisture flux within the HBL, among which the momentum fluxes had been able to capture the inertial subrange region, while moisture and heat flux cospectra has not able to capture the -5/3 slope. The turbulence spectral analysis of these physical parameters using WRF-LES data will provide valuable information and direction towards improvement in the SGS parametrization schemes.

The measurements of various terms in the turbulent kinetic energy budget imply that the major source/sink terms of the turbulent kinetic energy are the shear production and advection terms. But much of the shear production is compensated for by advection due to the strong hurricane winds and inhomogeneity. The TKE budget indicates that the contribution of buoyancy and pressure transport terms are not very significant within HBL. The least measured/observed advection term is very significant and acts as TKE source in the upper level of HBL.

The effect of SGS turbulence eddies on the hurricane intensity has been investigated by comparing the gradient of stress tensors computed explicitly and by using the Smagorinsky-2D, Smagorinsky-3D and TKE-1.5 order turbulence parameterization schemes respectively. The magnitude of gradient of stress tensor $\frac{\partial \tau_{ij}}{\partial x_j}$ on horizontal planes estimated explicitly are two order larger than that of the turbulence parameterization schemes. When the azimuthal average was taken, the parameterization schemes produce momentum sources/sinks in the same order as the explicit SFS turbulence. In the radial direction, the explicit SFS turbulence diffusion decelerates the radial inflow in surface layer and accelerates the radial outflow above it. In contrast, the TKE-1.5 order closure scheme produce too much turbulence dissipation on the azimuthal wind, the 3D smagorinsky scheme matches the magnitude of the explicit value, but it fails to generate positive tendency above the surface layer.

The estimated value of horizontal mixing length scale $l_h \sim 750m$ has been computed using explicit SFS turbulence and it is found to be consistent with the l_h value found by Rotunno and Bryan (2012) and also with the l_h value estimated using aircraft observations

(Zhang and Montgomery, 2012).

To summarize the thesis, the intensity and structure of the simulated hurricane is very sensitive to the specification of the l_h and Δx, are significantly different from the parametrized turbulence stresses. The spectra and co-spectra estimated from the wind, heat and moisture fields in the LES of an idealized hurricane show that the energetic eddies which have extracted the energy from the mean flow are $\sim 3km$ in size. A reasonable value of estimated mixing length scale $l_h \sim 750m$ should be used in order to improve hurricane forecasting accuracy of the operational forecasting models. Irrespective of the increase in the model resolution and change in turbulence mixing length scales, it seems that high resolution modelling is not able to resolve effectively the large turbulent eddies between $\sim 750m - 3km$ in size, because the forecasting of real-case Hurricane Danielle(2010) is not improve significantly with a high-resolution or a variation in the turbulence mixing length scale. This suggests that we need to improve the parameterization schemes and need a thorough understanding of turbulence characteristics and their effect on hurricane intensity prediction. Turbulence is not solely responsible for the prediction of hurricane and there are other factors which are responsible for controlling the hurricane intensity.

5.1 Future Scope

The boundary layer turbulence is an important factor in overall hurricane dynamics which plays a key role in determining the intensity and structure of the hurricane. However, it has not been thoroughly investigated due to a lack of thorough understanding of dynamics and physics within HBL and direct observations of HBL. The inefficiency of the numerical models to do accurate forecasting of hurricanes with increasing resolution noted here might be related to deficiencies in the sub-grid scale models. The current study also shows that the role of SFS turbulence plays a very significant role within HBL. The current boundary layer schemes significantly overestimate the HBL turbulent transport apparently due to the fact that the parameterizations do not have a very robust mechanism to include the effects of the SFS turbulence.

An avenue for the future research is to study the role of turbulence in the hurricane intensity by modifying the current turbulence parameterization schemes or developing new parameterization schemes. Following are a few suggestions which could be focused more in the near future to improve the hurricane intensity forecasting;

1. Dynamic Smagorinsky model: One major drawback of the eddy viscosity subgrid scale stress models (*current parameterization schemes in WRF-ARW model*) is their over-reliance on a Smagorinsky constant C_s and their inefficiency to represent the effects of turbulent accurately in a hurricane environment. An eddy viscosity model developed by Germano et al. (1991) which overcomes many of these drawbacks of the schemes *viz. backscatter-energy cascade, reliance on C_s, too much dissipation of energy etc.* In the Dynamic Smagorinsky model, the model coefficient is computed dynamically as the calculation progresses rather than input `apriori` (Germano et al., 1991). This model's performance found to be reasonably better than the current WRF-ARW turbulence models (Smagorinsky-2D and Smagorinsky-3D) (Kirkpatrick et al., 2006). The Dynamic Smagorinsky model can be implement into WRF-ARW model to evaluate the accuracy of the hurricane intensity forecasting.

2. Testing of LEC model suggested by Zhu (2008) showed that current parameterization schemes do not have a mechanism to include the effect of hurricane boundary

layer Large Eddy Circulations. He proposed a updraft-downdraft statistical model which can be used to develop parameterizations that can be potentially implemented in weather forecasting models to parameterize the fluxes induced by the HBL LECs. Model proposed by Zhu (2008), can be developed and test for hurricane environment.

References

Ahmed, N., and K. R. Rao, 1974: Discrete cosine transform. *IEEE Transactions on Computers*, **C-23**, 90–93.

AMS-Council-March, 2007: Hurricane forecasting in the united states: An information statement of the american meteorological society. *Bull. Am. Meteor. Soc.*, **88**, 1–2.

Anderson, D., K. I. Hodges, and B. J. Hoskins, 2003: Sensitivity of feature based analysis methods of storm tracks to the form of background field removal. *Mon. Wea. Rev.*, **131**, 565–573.

Benjamin, W. S., and F. Zhang, 2013: Impacts of airsea flux parameterizations on the intensity and structure of tropical cyclones. *American Meteorological Society*, **141**, 2308–2324.

Black, P. G., E. A. D'Asaro, W. M. Drennan, J. R. French, P. P. Niiler, T. B. Sanford, E. J. Terrill, E. J. Walsh, and J. A. Zhang, 2007: Air-sea exchange in hurricanes: Synthesis of observations from the coupled boundary layer air-sea transfer experiment. *Bull. Am. Meteor. Soc.*, **88**, 357–374.

Braun, S. A., and W. K. Tao, 2000: Sensitivity of high-resolution simulations of hurricane bob (1991) to planetary boundary layer parameterizations. *Mon. Wea. Rev.*, **128**, 3941–3961.

Bryan, G. H., and R. Rotunno, 2009a: The influence of near-surface, high-entropy air in hurricane eyes on maximum hurricane intensity. *J. Atmos. Sci.*, **66**, 148–158.

Bryan, G. H., and R. Rotunno, 2009b: The maximum intensity of tropical cyclones in axisymmetric numerical model simulations. *Mon. Wea. Rev.*, **137**, 1770–1789.

Caughey, J., and J. C. Wyngaard, 1979: The turbulent kinetic energy budget in convective conditions. *Quarterly Journal of Royal Meteorological Society*, **105**, 231–239.

Davis, C., and Coauthors, 2008: Prediction of landfalling hurricanes with the advanced hurricane wrf model. *Mon. Wea. Rev.*, **136**, 1990–2005.

Deardorff, J. W., 1970: A numerical study of three dimensional turbulent channel flow at lare reynolds numbers. *Journal of Fluid Mechanics*, **41**, 453.

Denis, B., J. Côtè, and R. Laprise, 2002: Spectral decomposition of 2d atmospheric fields on limited-area domains using the discrete cosine transform(dct). *Mon. Wea. Rev.*, **130**, 1812–1829.

Emanuel, K. A., 1997: Some aspects of hurricane inner-core dynamics and energetics. *J. Atmos. Sci.*, **54**, 1014–1026.

Emanuel, K. A., 2005: Increasing destructiveness of tropical cyclones over the past 30 years. *Nature*, **436**, 686–688.

Erico, R. M., 1985: Spectra computed from a limited area grid. *Mon. Wea. Rev.*, **113**, 1554–1563.

Feser, F., and H. von Storch, 2005: A spatial two-dimensional discrete filter for limited-area-model evaluation purposes. *Mon. Wea. Rev.*, **133**, 1774–1786.

Frenzen, P., and C. A. Vogel, 1992: The turbulent kinetic energy budget in the atmospheric surface layer: a review and an experimental reexamination in the field. *Boundary Layer Meteorology*, **60**, 49–76.

Germano, M., U. Piomelli, M. Parviz, and W. H. Cabot, 1991: A dynamic subgrid?scale eddy viscosity model. *Physics of Fluids*, **A3**, 1760–1771.

Hock, T. F., and J. L. Franklin, 1999: The ncar gsp dropwindsonde. *Bull. Am. Meteor. Soc.*, **80**, 407–420.

Holza, F., and R. E. Robins, 2004: Probabilistic two-phase aircraft wake vortex model: application and assessment. *Journal of Aircraft*, **41, no. 5**, 1117–1126.

Hoskins, B. J., and K. I. Hodges, 2002: New perspectives on northern hemisphere storm tracks. *J. Atmos. Sci.*, **59**, 1041–1061.

Kaimal, J. C., and J. J. Finnigan, 1994: *Atmospheric Boundary Layer Flows*. Oxford University Press, 304 pp.

Kaimal, J. C., J. C. Wyngaard, Y. Izumi, and O. R. Cote, 1972: Spectral characteristics of surface-layer turbulence. *Quart. J. Roy. Meteor. Soc.*, **98**, 563–589.

Kain, J. S., and J. M. Fritsch, 1990: A one-dimensional entraining/detraining plume model and its application in convective parameterization. *J. Atmos. Sci.*, **47**, 2784–2802.

Kepert, J. D., 2006: Observed boundary layer wind structure and balance in the hurricane core. part i: Hurricane georges. *J. Atmos. Sci.*, **63**, 2169–2193.

Kirkpatrick, M. P., A. S. Ackerman, D. E. Stevens, and N. N. Mansour, 2006: On the application of the dynamic smagorinsky model to large-eddy simulations of the cloud-topped atmospheric boundary layer. *J. Atmos. Sci.*, **63**, 526–546.

Kuo, H. L., 1971: Axisymmetric flows in the boundary layer of a maintained vortex. *J. Atmos. Sci.*, **28**, 20–41.

Laursen, L., and E. Eliasen, 1989: On the effects of the damping mechanisms in an atmospheric general circulation model. *Tellus*, **41A**, 385–400.

Leonard, A., 1974: Energy cascade in large eddy simulation of turbulent fluid flow. *Adv. Geophys*, **18A**, 237–248.

Li, S., 2012: *A Study on the Turbulent Characteristics within the Hurricane Boundary Layer*. PhD thesis, University of Western Ontario, Ontario, Canada.

Lilly, D. K., 1966: The representation of small-scale turbulence in numerical simulation experiments. *NCAR Manuscript*, **281**, –.

Lorsolo, S., J. Zhang, F. M. Jr., and J. Gamache, 2010: Estimation and mapping of hurricane turbulent energy using airborne doppler measurements. *Mon. Wea. Rev.*, **138**, 3656–3670.

Marks, J. F. D., and R. A. Houze, 1987: Inner core structure of hurricane alicia from airborne doppler radar observations. *J. Atmos. Sci.*, **44**, 1296–1317.

Mason, P., and D. Thompson, 1992: Stochastic backscatter in large-eddy simulations of boundary layers. *J. Fluid Mech.*, **242**, 51–78.

Miglietta, M. M., and R. Rotunno, 2005: Numerical simulations of nearly moist neutral flow past a two-dimensional ridge. *J. Atmos. Sci.*, **62**, 1410–1427.

Montgomery, M. T., N. V. Sang, R. K. Smith, and J. Persing, 2009: Do tropical cyclones intensify by wishe? *J. Roy. Meteor. Soc.*, **135**, 1697–1714.

Ooyama, K., 1969: Numerical simulation of the life cycle of the tropical cyclones. *J. Atmos. Sci.*, **26**, 3–40.

Persing, J., and M. T. Montgomery, 2003: A multiscale numerical study of hurricane andrew (1992). part vi: Small-scale inner-core structures and wind streaks. *J. Atmos. Sci.*, **60**, 2349–2371.

Piomelli, U., and E. Balaras, 2002: Wall-layer models for large-eddy simulations. *Annual Review of Fluid Mechanics*, **34**, 349–374.

Pope, S. B., 2000: *Turbulent Flows*. Cambridge University Press.

Rosenbaum, S., 2006: United states health policy in the aftermath of hurricane katrina. *Jama-Journal of the American Medical Association*, **4**, 437–440.

Rotunno, R., and G. H. Bryan, 2012: Effects of parameterized diffusion on simulated hurricanes. *American Meteorological Society*, **69**, 2284–2299.

Rotunno, R., Y. Chen, W. Wang, C. Davis, J. Dudhia, and G. J. Holland, 2009: Large-eddy simulation of an idealized tropical cyclone. *Bull. Am. Meteor. Soc.*, **90**, 1783–1788.

Rotunno, R., and K. A. Emanuel, 1987: An air-sea interaction theory for tropical cyclones. part ii: Evolutionary study using a nonhydrostatic axisymmetric numerical models. *J. Atmos. Sci.*, **44**, 542–561.

Schlichting, H., 1996: *Boundary-Layer Theory*. McGraw-Hill, 6th Ed., 748 pp.

Schroeder, J. L., B. P. Edwards, and I. M. Giammanco, 2009: Observed tropical cyclone wind flow characteristics. *Wind and Structures*, **12**, 349–381.

Shapiro, R., 1975: Linear filtering. *Mathematics of Computation*, **29(132)**, 1094–1097.

Skamarock, W. C., J. B. Klemp, J. Dudhia, D. O. Gill, B. M. Dale, M. G. Duda, X.-Y. Huang, W. Wei, and J. G. Powers, 2008: A description of the advanced research wrf version 3.0. *NCAR Technical Note*, **NCAR/TN-475+STR**, 1–113.

Smagorinsky, J., 1963: General circulation experiments with the primitive equations i. the basic experiment. *Mon. Wea. Rev.*, **91**, 99–164.

Southern, R. L., 1979: The global socio-economic impact of tropical cyclones. **27**, 175–195.

Stevens, B., and D. Lenschow, 2001: Observations, experiments, and large eddy simulation. *Bull. Am. Meteor. Soc.*, **82**, 283–294.

Stull, R., 1988: *An introduction to Boundary Layer Meteorology*. Kluwer Academic Publishers.

Tuleya, R. E., and Y. Kurihara, 1978: Low-level turbulence structure in the vicinity of a hurricane. *Mon. Wea. Rev.*, **106**, 841–849.

Tyagi, B., and A. N. V. Satyanarayana, 2013: The budget of turbulent kinetic energy during premonsoon season over kharagpur as revealed by storm experimental data. *ISRN Meteorology*, **Volume(2013)**, 1–12.

Vickery, P. J., D. Wadhera, M. D. Powell, and Y. Chen, 2009: A hurricane boundary layer and wind field model for use in engineering application. *J. Appl. Meteor. Climatol*, **48**, 381–405.

Winckelmans, G. S., T. S. Lund, D. Carati, and A. Wray, 1996: *A priori testing of subgrid-scale models for the velocity-pressure and vorticity-velocity formulations*. Proceedings of the Summer Program - Center for Turbulence Research, 309–329 pp.

Wyngaard, J. C., 2004: Toward numerical modeling in the terra incognita. *J. Atmos. Sci.*, **61**, 1816–1826.

Yanai, M., 1964: Formation of tropical cyclones. *Rev. Geophysics*, **2**, 367–414.

Yau, M. K., Y. Liu, D. L. Zhang, and Y. Chen, 2004: A multiscale numerical study of hurricane andrew (1992). part vi: Small-scale inner-core structures and wind streaks. *Mon. Wea. Rev.*, **132**, 1410–1433.

Yu, B., A. G. Chowdhury, and F. J. Masters, 2008: Hurricane wind power spectra, cospectra, and integral length scales. *Boundary-Layer Meteorol.*, **129**, 411–430.

Zhang, J., 2007: *An Airborne Investigation of the Atmospheric Boundary Layer Structure in the Hurricane Force Wind Regime*. University of Miami, Scholarly Repository, Ph.D. Thesis.

Zhang, J. A., 2010: Spectral characteristics of turbulence in the hurricane boundary layer over the ocean between the outer rain bands. *Quart. J. Roy. Meteor. Soc.*, **136**, 918–926.

Zhang, J. A., and M. T. Montgomery, 2012: Observational estimates of the horizontal eddy diffusivity and mixing length in the low-level region of intense hurricanes. *American Meteorological Society*, **69**, 1306–1316.

Zhu, P., 2008: Simulation and parameterization of the turbulent transport in the hurricane boundary layer by large eddiess. *J. Geophys. Res.*, **113**, D17.